

Electron probe microanalysis of thin films and multilayers

X. Llovet

University of Barcelona, Spain

C. Merlet

University of Montpellier II, France



Outlook:

- Introduction
- Electron-specimen interactions. X-ray generation
- Quantitative analysis: bulk samples
- Quantitative analysis: thin films and multilayers
- Practical aspects
- Examples

● **Electron Probe Microanalysis (EPMA)**

- Non-destructive technique used for determining the “local” composition of solid samples
- The basis of quantitative analysis and the first electron microprobe instrument were developed by Raimond Castaing (1951)
- Composition is obtained from the measurement of characteristic x-ray intensities emitted by the sample when it is bombarded with a focused electron beam.
- Transformation from measured x-ray intensities to concentrations is performed by means of relatively simple, analytical algorithms
- Conventional EPMA is suitable for the analysis of samples that are homogeneous at the micrometer scale.
- Thin films and multilayers can also be analyzed by EPMA.

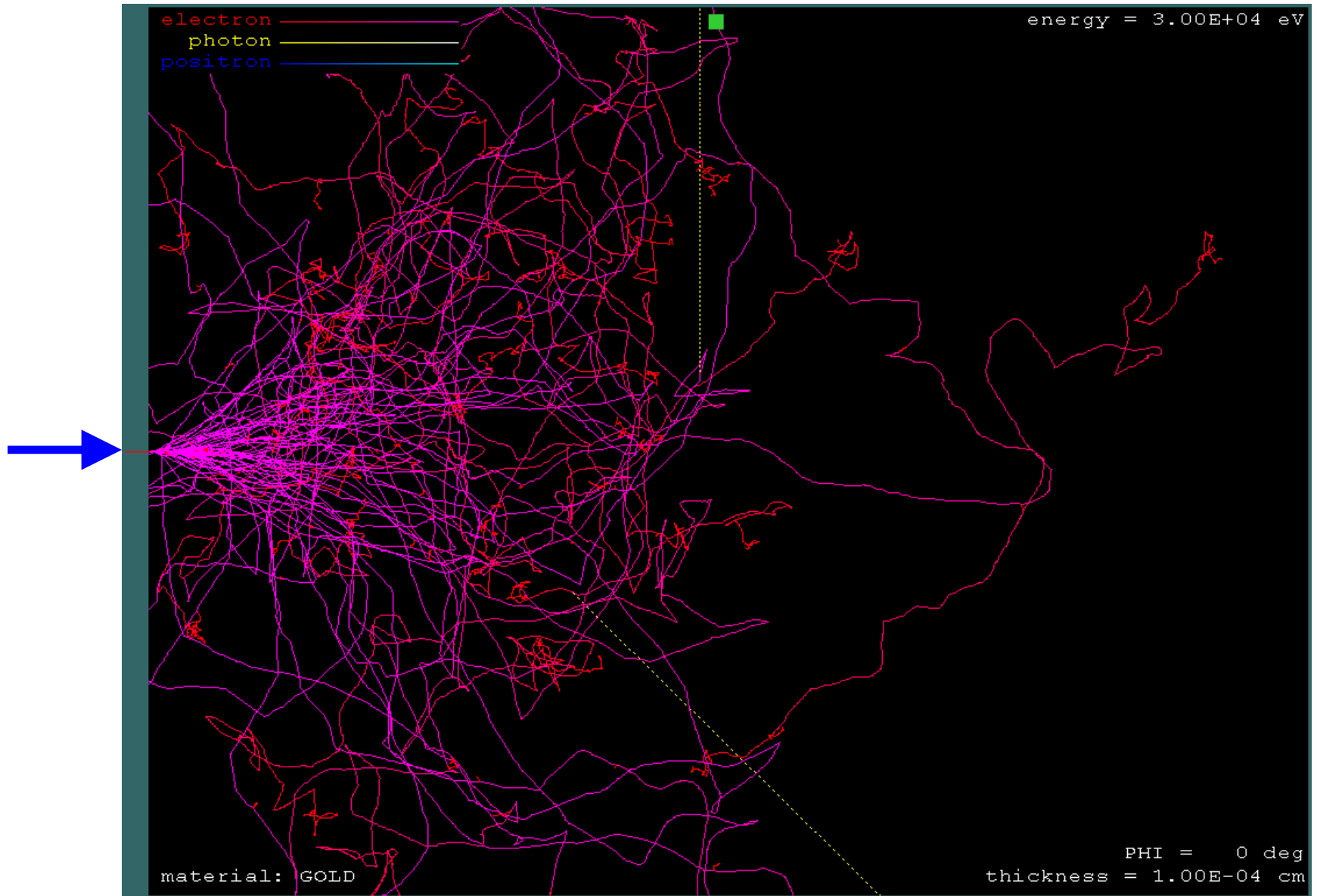
● Analysis of thin films and multilayers by EPMA

- First attempts: empirical methods, based on calibration curves and thin-film standards (Cockett & Davies, 1963; Marshall & Hall, 1968..)
- Monte Carlo simulations: pioneering work of Kyser & Murata (1974)
- Systematic extension of EPMA algorithms (1980-1990's):
 - Pouchou & Pichoir (1984)
 - Packwood *et al* (1985-86)
 - Willich & Obertop (1988)
 - Bastin *et al* (1990-91)
 - Merlet (1995)

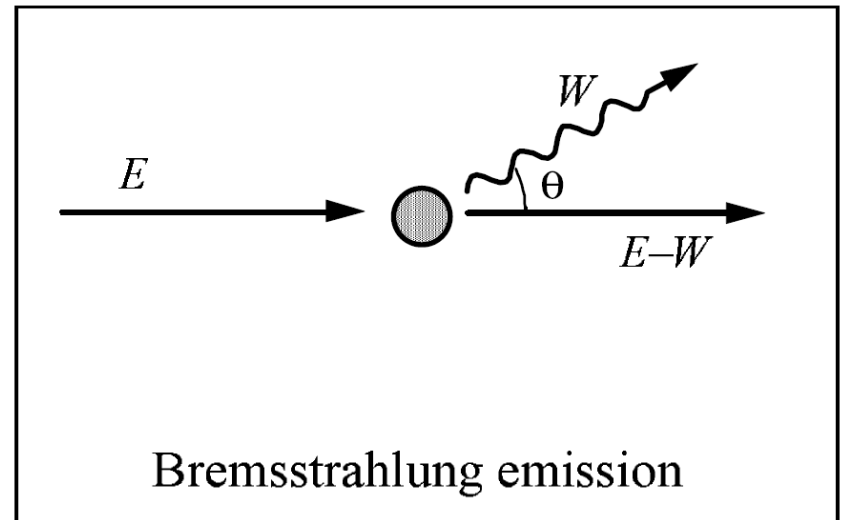
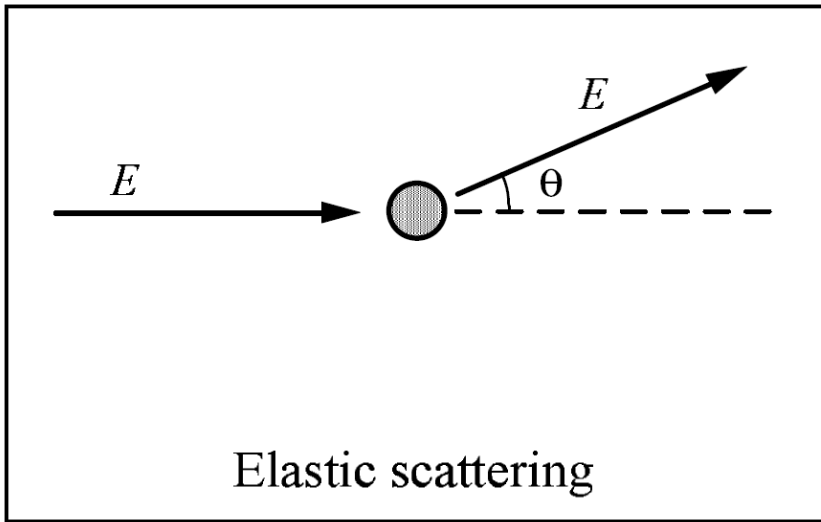
● Available today:

- Commercial programs:
 - LAYERF, STRATAgem (Pouchou & Pichoir)
 - TFA, MTFA (Bastin *et al.*)
 - XFILM (Merlet)
- Free software: GMRFilm (Waldo)
- Monte Carlo simulation codes: CASINO, WinXRay, PENELOPE...

● *Electron-specimen interactions*



● Electron scattering and bremsstrahlung emission



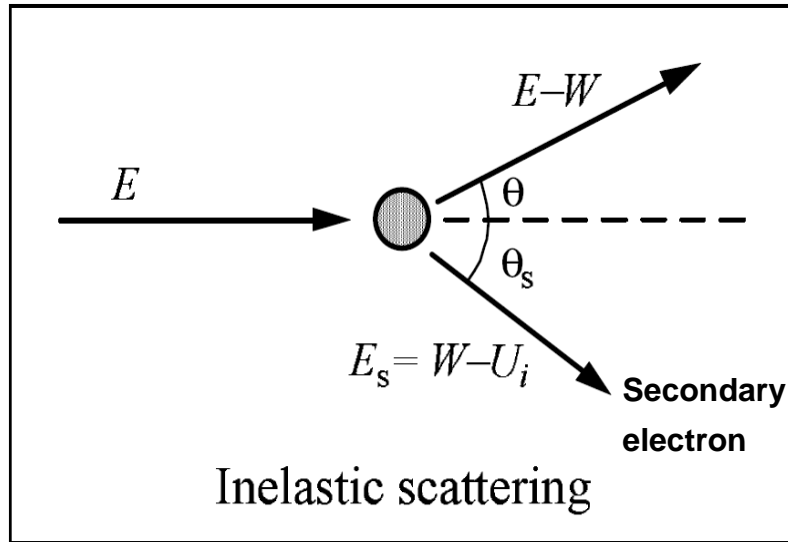
- Collisions without electronic excitation of the target.
- Deflection of the direction of movement of incident electron

θ = scattering angle

- Electrons are accelerated by the electrostatic field of the target atom and emit electromagnetic radiation

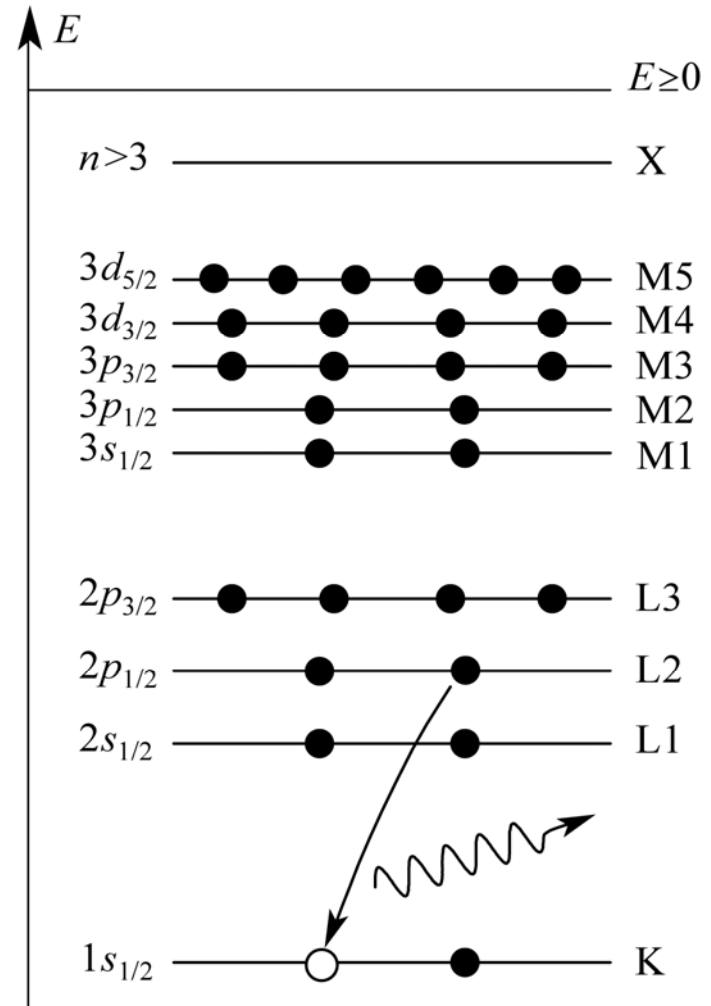
W = energy of the emitted photon
 θ = polar angle of the photon direction relative to the electron direction

● Inelastic scattering and atomic relaxation



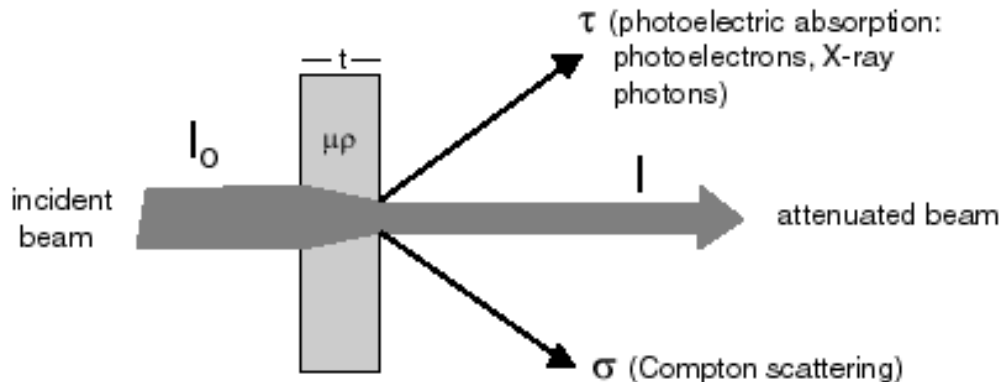
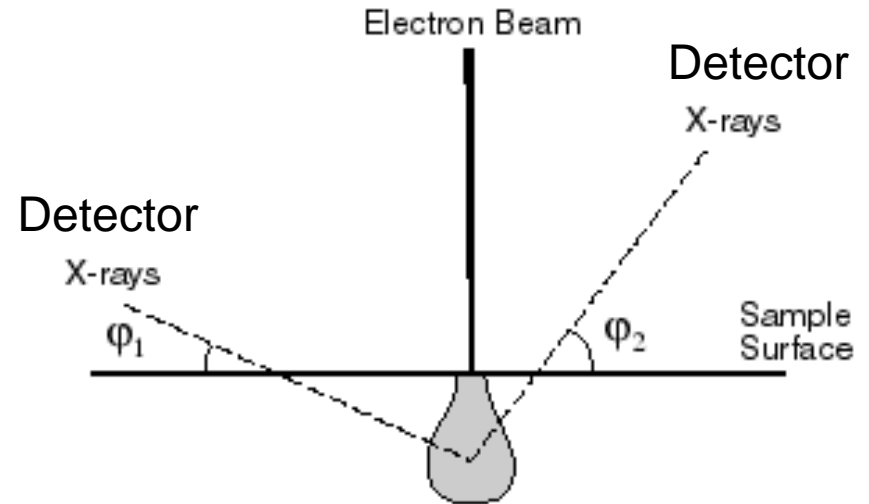
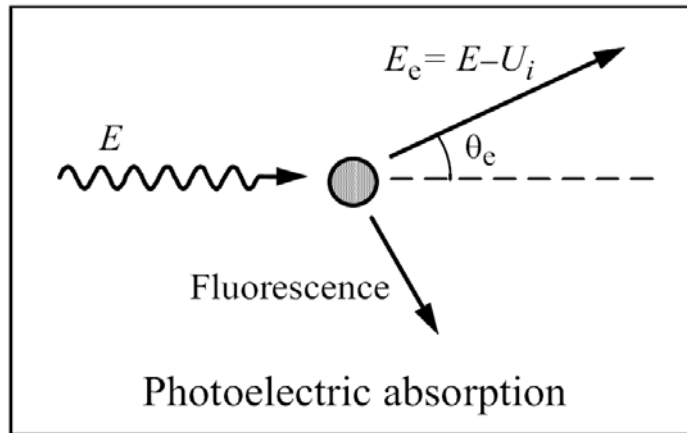
● Collisions that cause electronic excitation of the target:

- plasmon excitation
- outer-shell ionization
- inner-shell ionization



● After inner-shell ionization atomic relaxation causes the emission of x-rays or Auger electrons

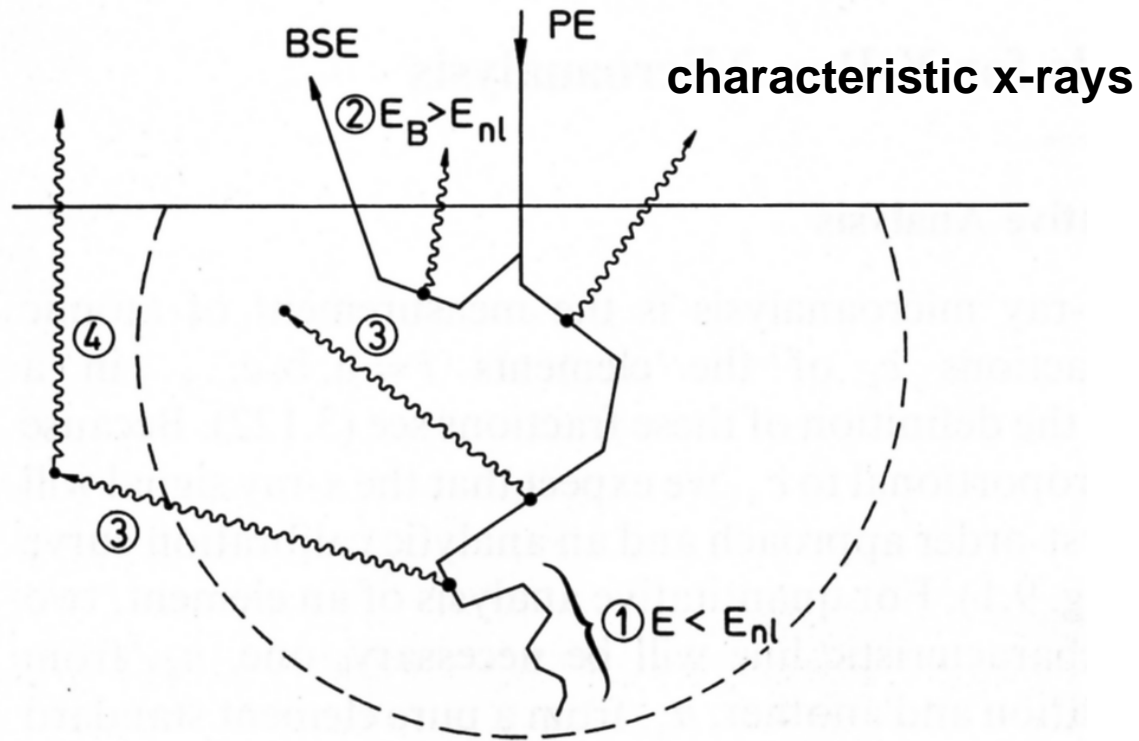
● Photon interactions



Take-off angle: direction of the detector with respect to the sample surface. It is typically in the range 35° - 45° .

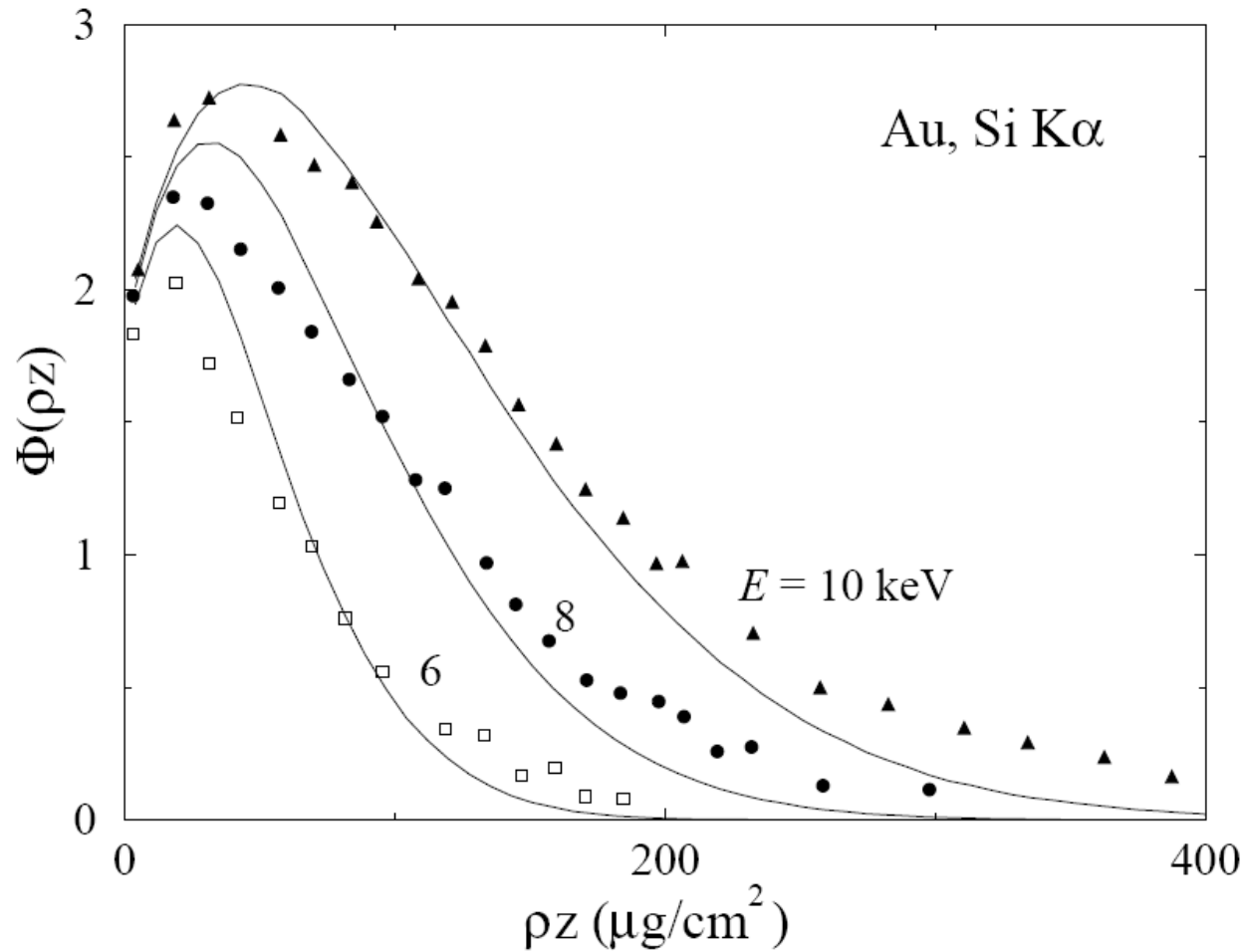
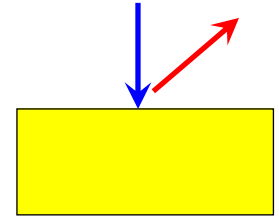
- Emitted x-rays can interact within the sample via photoelectric absorption and Compton scattering. The global global effect is **x-ray attenuation**

- **Effects influencing the x-ray emission:**



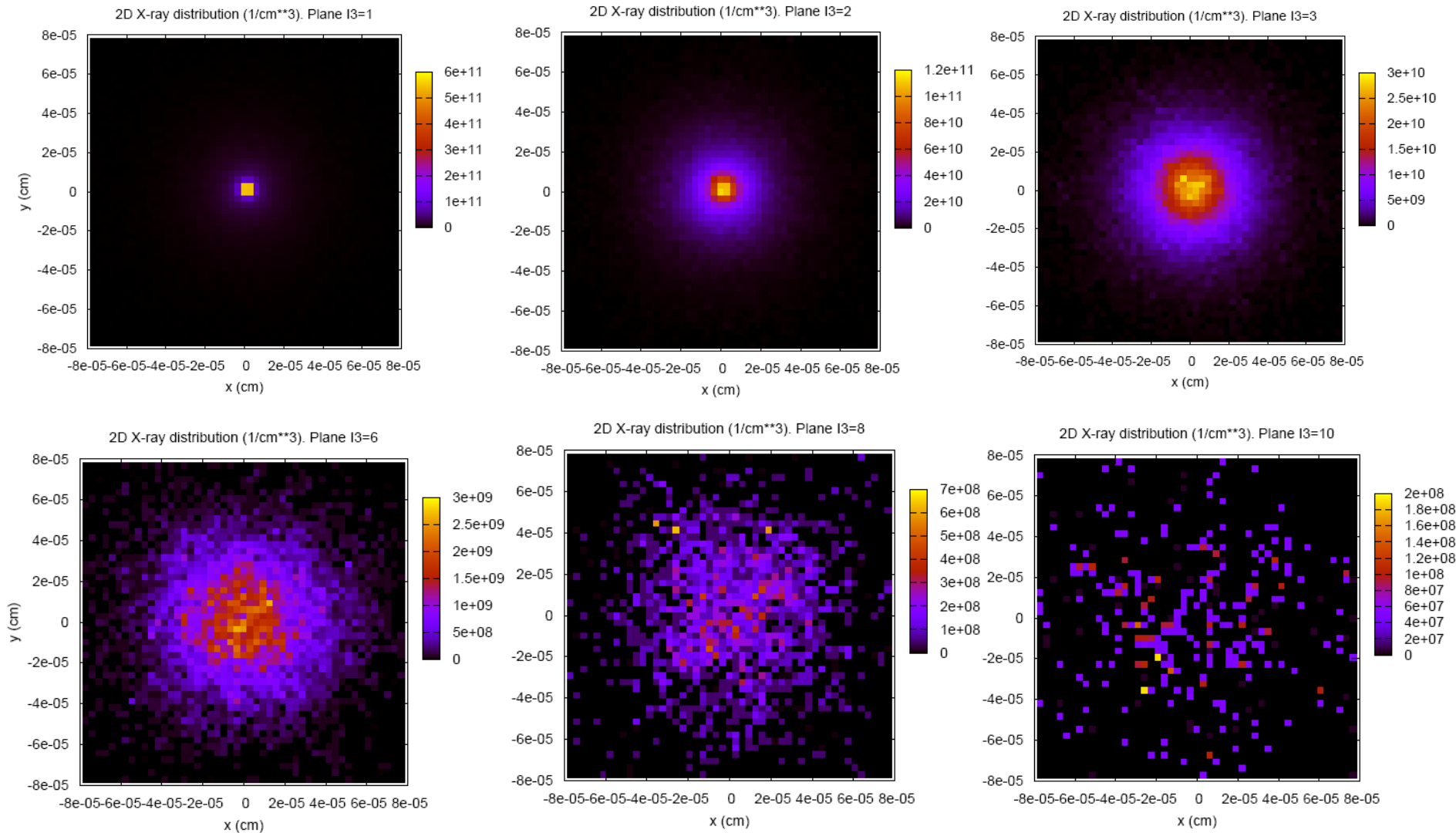
- 1) Electron with energy below the ionization threshold
- 2) Decrease of x-ray emission when backscattered electrons have energy above the ionization threshold
- 3) Photoelectric absorption
- 4) Fluorescence emission after photoelectric absorption

● *Depth-distribution of ionizations*



Depth distribution of ionizations for Si K α x-rays in Au at different energies
Comparison of Monte Carlo simulation using PENELOPE with experiments

● 2D depth-distribution of x-ray production



2-D depth distribution of x-ray emission for Pu $M\alpha$ x-rays from Pu at 25 keV.
Simulation results using PENELOPE

● Quantitative analysis. Bulk samples

Relation between the measured intensity and the concentration (element i):

$$I_i = \mathcal{A} c_i \left[\int_0^\infty \Phi_i(\rho z) \exp(-\chi_i \rho z) d(\rho z) \right] \mathcal{F}$$

concentration attenuation fluorescence correction
 characteristic x-ray intensity depth-distribution of ionizations $i = 1, \dots, N$
 $N =$ number of elements

$$\mathcal{A} = n_{\text{el}} (N_{\text{A}}/A_i) \epsilon \Omega / (4\pi) \omega_i p_i \sigma_i(E) (1 + T_{CK})$$

Instrumental and atomic factors

n_{el} = Number of electrons

ϵ = Detector efficiency

Ω = Solid angle

ω = Fluorescence yield

p = X-ray line emission rate

σ = Inner-shell ionization cross section

T = Coster-Kronig correction

$$\chi_i = (\mu/\rho)_i \csc \theta$$

Attenuation factor

μ = mass attenuation coefficient

ρ = density

θ = take-off angle

● Quantitative analysis. Bulk samples

K-ratio: measurements on reference standards

$$K_i = \frac{I_i}{I_i^*} = \frac{c_i}{c_i^*} \frac{\int_0^\infty \Phi_i(\rho z) \exp(-\chi_i \rho z) d(\rho z)}{\int_0^\infty \Phi_i^*(\rho z) \exp(-\chi_i^* \rho z) d(\rho z)} \frac{\mathcal{F}}{\mathcal{F}^*} \leftarrow \text{standard}$$

● Different parameterizations of $\phi(\rho z)$:

- Quadrilateral model (Love & Scott)
- Surface-centered Gaussian (Packwood & Brown, Bastin *et al.*)
- Parabolic model (Pouchou & Pichoir)
- Double-Gaussian model (Merlet, Bastin *et al.*)

● MACs': Heinrich, Henke, XCOM, FFAST, etc..

1) K-ratios are obtained for each element (except for those estimated by stoichiometry or other means)

2) The system of equations is solved by using an iterative procedure

[$\phi(\rho z)$ and χ also depend on c_i]

➔ Relative accuracies better than 2% can be achieved

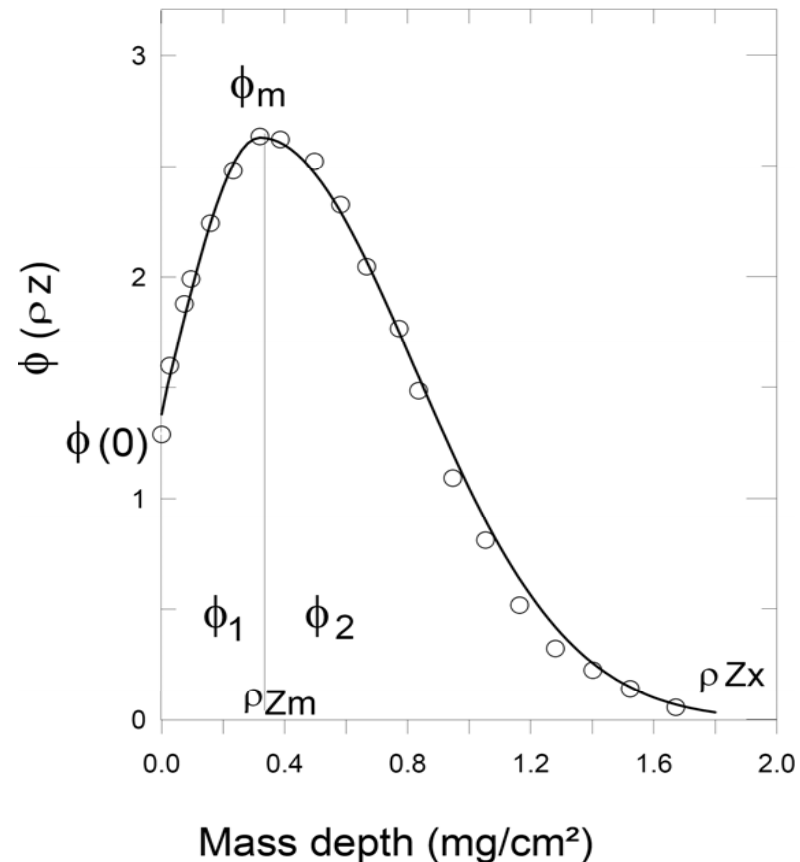
● The X-PHI model

- Merlet (1992)
- Double Gaussian model: 2 branches
 ϕ_1 and ϕ_2 joined at the maximum
- Characterized by 4 parameters:
 - $\phi(0)$: surface ionization
 - ϕ_m : maximum
 - ρz_m : depth of the maximum
 - ρz_x : x-ray range
- X-ray intensity: obtained analytically

$$\Phi_1 = \Phi_m \exp \left[- \left(\rho z - \rho z_m \right)^2 / \beta^2 \right] \quad \text{for } 0 < \rho z < \rho z_m$$

$$\Phi_2 = \Phi_m \exp \left[- \left(\rho z - \rho z_m \right)^2 / \alpha^2 \right] \quad \text{for } \rho z_m < \rho z < \rho z_x$$

$$\alpha = 0.46598 (\rho z_x - \rho z_m) \quad \beta = \rho z_m \frac{\ln(\Phi_m)}{\sqrt{\Phi(0)}}$$



Depth-distribution of ionizations for Al K α in Cu. Comparison of the predictions of X-PHI with the experimental data of Castaing & Henoc (1965)

- **Quantitative analysis. Thin films & multilayers**

- Thin films on substrates:

$$I_{Fi} = \mathcal{A} c_i \left[\int_0^t \Phi_{Fi}(\rho z) \exp(-\chi_{Fi} \rho z) d(\rho z) \right] \mathcal{F}_F \quad \text{film} \quad \text{substrate}$$

$$I_{Sj} = \mathcal{A} c_j \exp[(\chi_{Sj} - \chi_{Fj}) t] \left[\int_t^\infty \Phi_{Si}(\rho z) \exp(-\chi_{Sj} \rho z) d(\rho z) \right] \mathcal{F}_S$$

- Multilayer films:

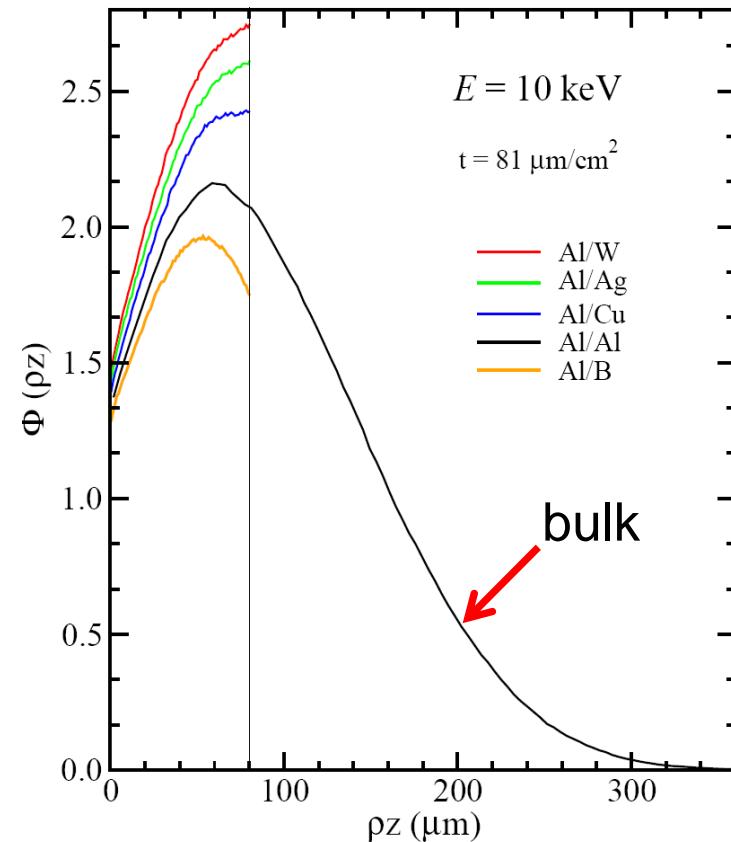
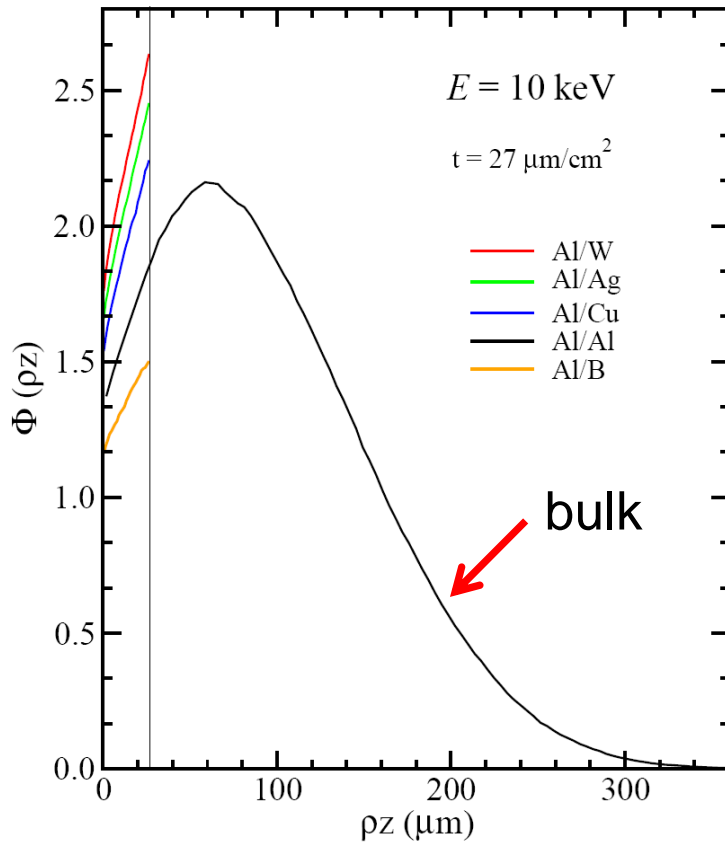
$t =$ mass thickness of the layer

$$I_{ki} = \mathcal{A} c_i \prod_{j=1}^{k-1} \exp[-(\chi_{ki} - \chi_{ji}) T_j] \left[\int_{t_k}^{t_{k+1}} \Phi_{ki}(\rho z) \exp(-\chi_{ki} \rho z) d(\rho z) \right] \mathcal{F}_k$$

$k = 1, \dots, \text{number layers}$

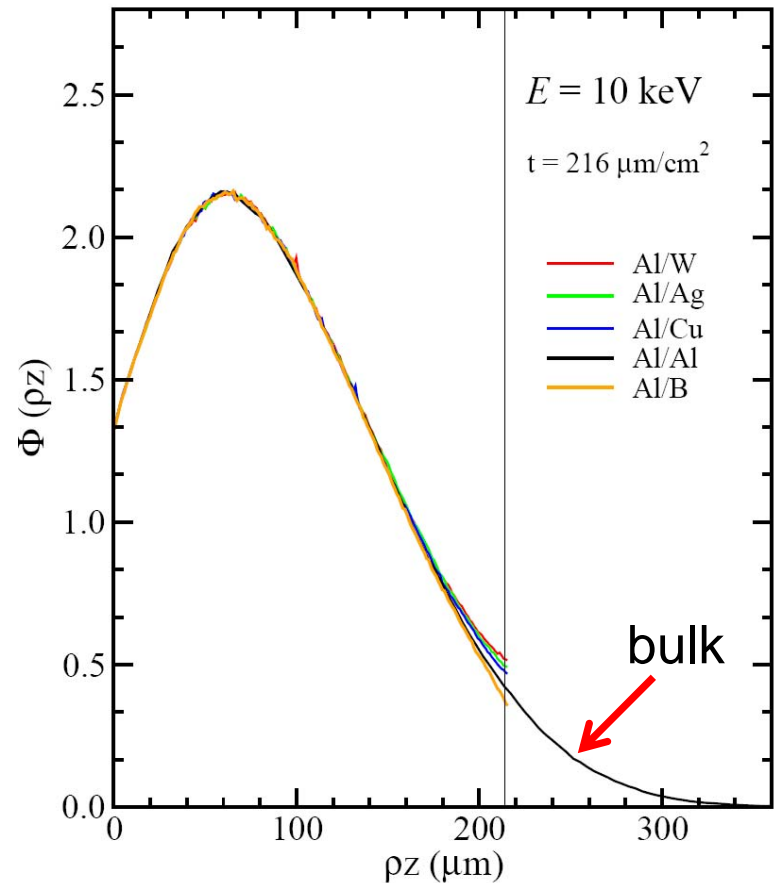
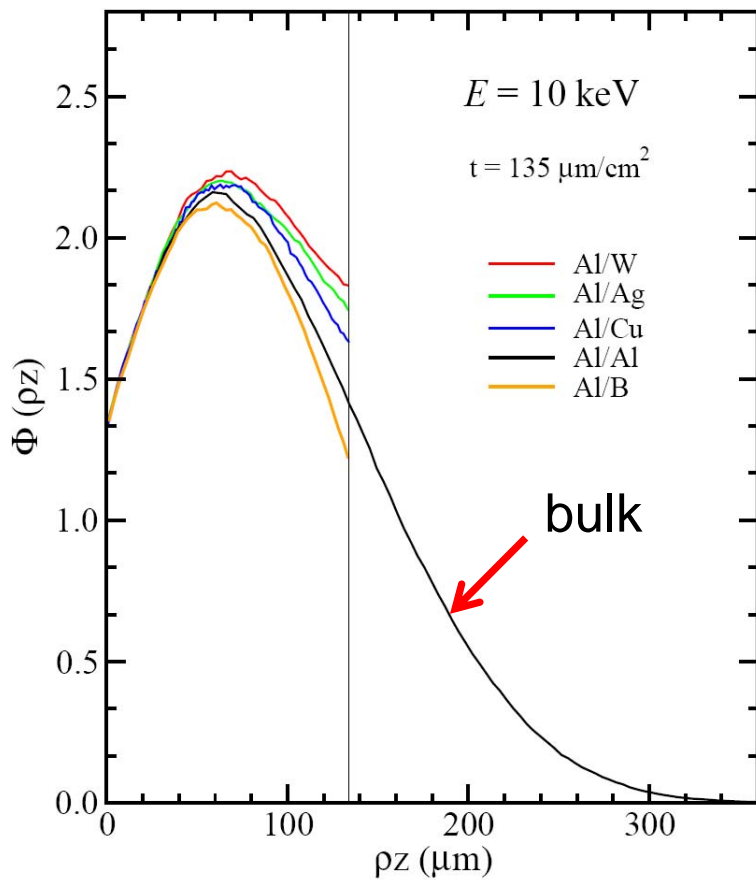
- K -ratio measurements performed at varying incident electron energy (variable-voltage EPMA)
- Systems of equations solved by using iterative procedure: values of composition and thickness that best match the experimental data are obtained

● Depth-distribution of ionizations for thin films



- Number of ionizations increases for increasing Z of substrate
- Differences between film-bulk are larger at the interface
- For relatively thin films, the surface ionization increases for increasing Z of substrate

● Depth-distribution of ionizations for thin films



- For intermediate thicknesses: shift of the maximum to larger depths
- For relatively thick films, backscattered electrons are absorbed in the film (surface ionization not affected)

● Some difficulties:

- System of equations more difficult to solve than for bulk samples:
 - Additional variables (thickness)
 - Elements can be present simultaneously in different layers
- Convergence to a unique solution is not guaranteed, especially if:
 - The structure of the layers is not known
 - X-rays from buried layers do not emerge due to strong absorption
- ✓ Large number of voltage measurements (to check consistency)
- ✓ Use of different x-ray lines for the same element
- ✓ Accurate initial values of estimations (concentration, thickness)
- ✓ Data processing by trial-error procedure (simulation mode)
- Analytical predictions not firmly established for multilayer films with adjacent layers with large differences in Z
 - ✓ Suitable selection of electron incident energies

Nevertheless, in extreme situations, the composition and thickness may not be obtainable only by EPMA

● The X-FILM model

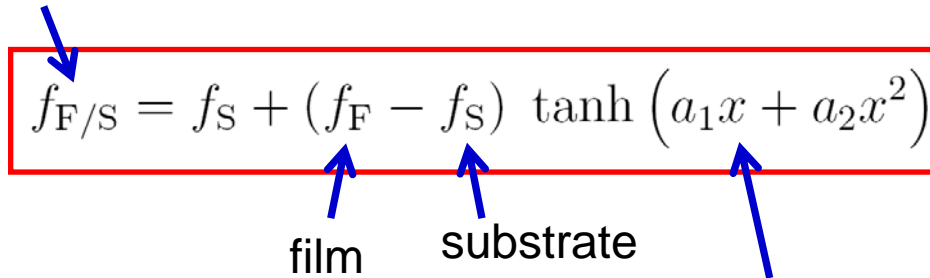
Merlet (1994): extension of X-PHI for thin-film analysis

Assumptions:

- $\phi_{F/S}(\rho z)$ described by a “weighted” combination of $\phi_F(\rho z)$ and $\phi_S(\rho z)$
- $\phi_{F/S}(\rho z)$: corresponds to a fictitious bulk sample with parameters calculated using an empirical “weighting” rule

Weighting rule (Hunger & Rogaschewski, 1984)

film-substrate

$$f_{F/S} = f_S + (f_F - f_S) \tanh(a_1 x + a_2 x^2)$$


film

substrate

a_1, a_2 : parameters

reduced thickness

$$x = 4t/\rho z_x$$

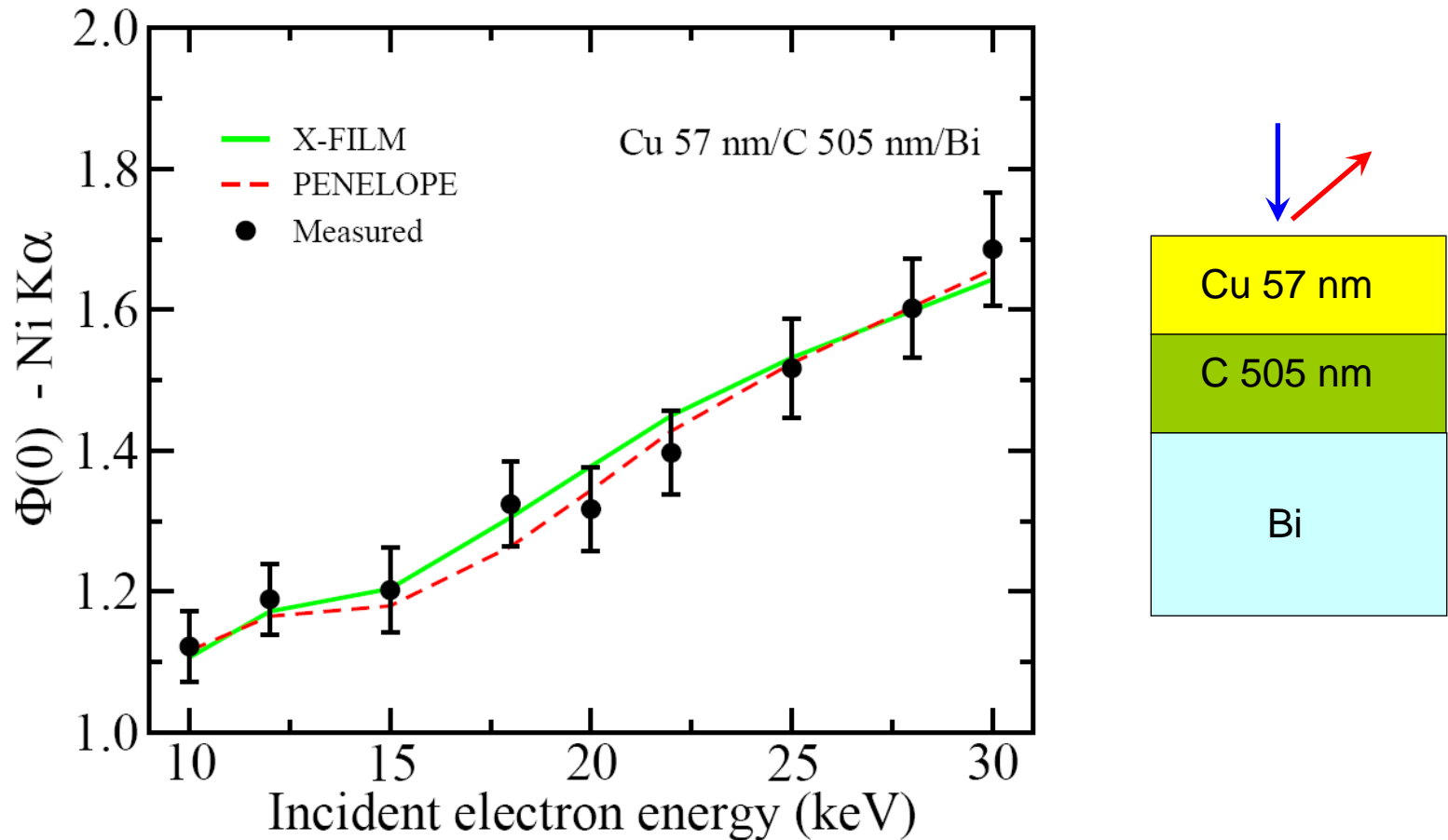
Applied to all parameters:

$$f = \Phi(0), \Phi_m, \rho z_m \text{ and } \rho z_x$$

Other thin-film programs: similar assumptions, with different weighting rules

Difficulties: experimental measurements of $\phi_{F/S}(\rho z)$ scarce

- **The X-FILM model: surface ionization from multilayers**



- The “weighting” rule of Hunger & Rogachewsky describes satisfactorily the surface ionization from multilayer films, even for adjacent layers with very different Z

● The X-FILM model: emitted x-ray intensity

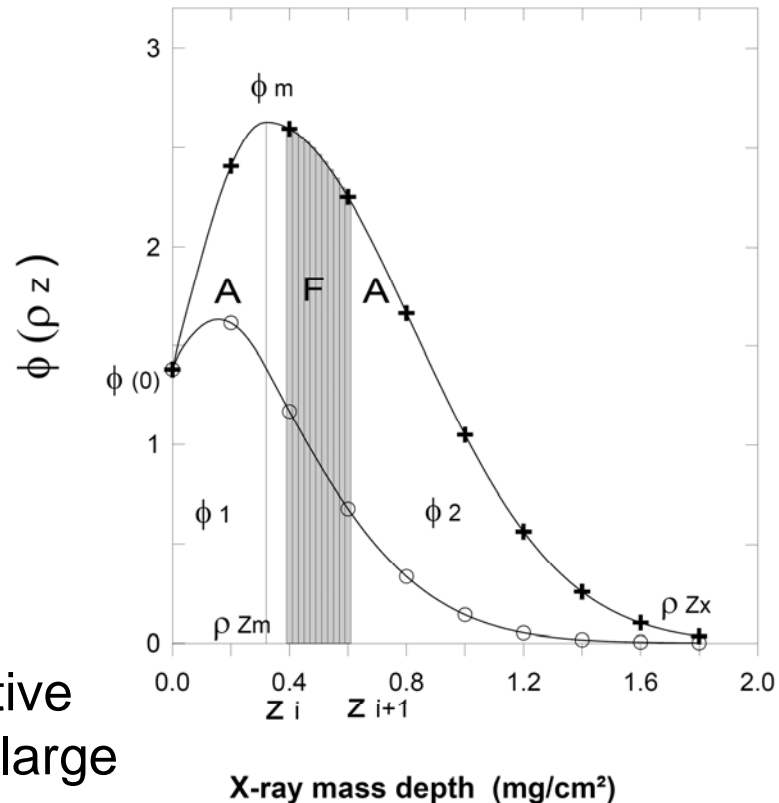
X-ray intensity can be computed analytically:

$$I_{ki} = \frac{\mathcal{A} c_i \Phi_m \zeta \sqrt{\pi}}{2} \exp(b) \prod_{j=1}^{k-1} \exp[-(\chi_{ki} - \chi_{ji}) T_j] \left[\operatorname{erf} \left(\frac{t_{k+1} - \delta}{\zeta} \right) - \operatorname{erf} \left(\frac{t_k - \delta}{\zeta} \right) \right]$$

$$\text{with: } \zeta = \begin{cases} \alpha & \text{for } 0 < \rho z < \rho z_m \\ \beta & \text{for } \rho z_m < \rho z < \rho z_x \end{cases}$$

$$b = [(\zeta \chi_{ki})/2]^2 - \rho z_m \chi_{ki}$$

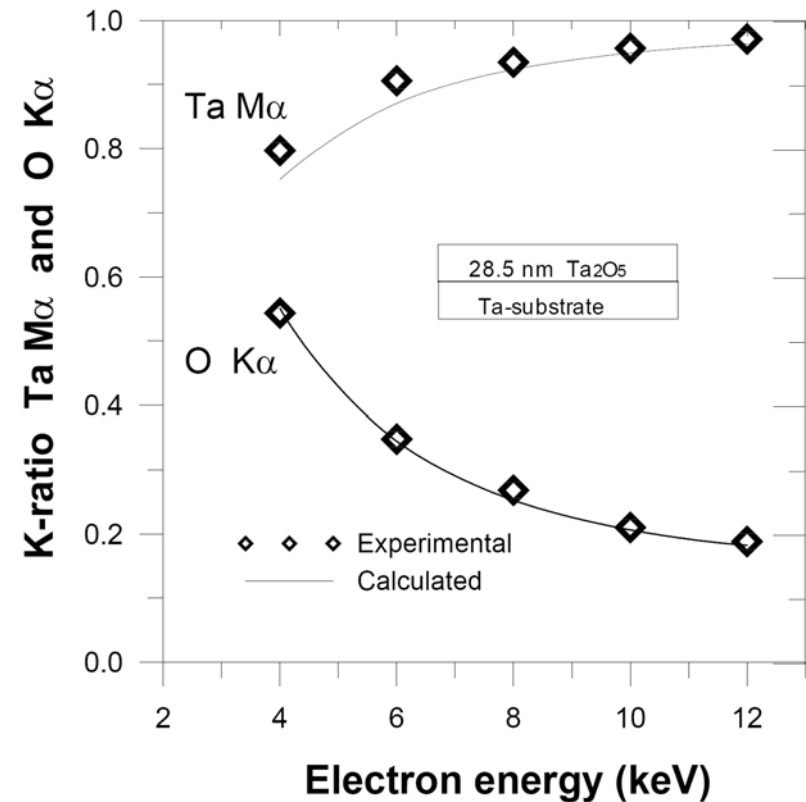
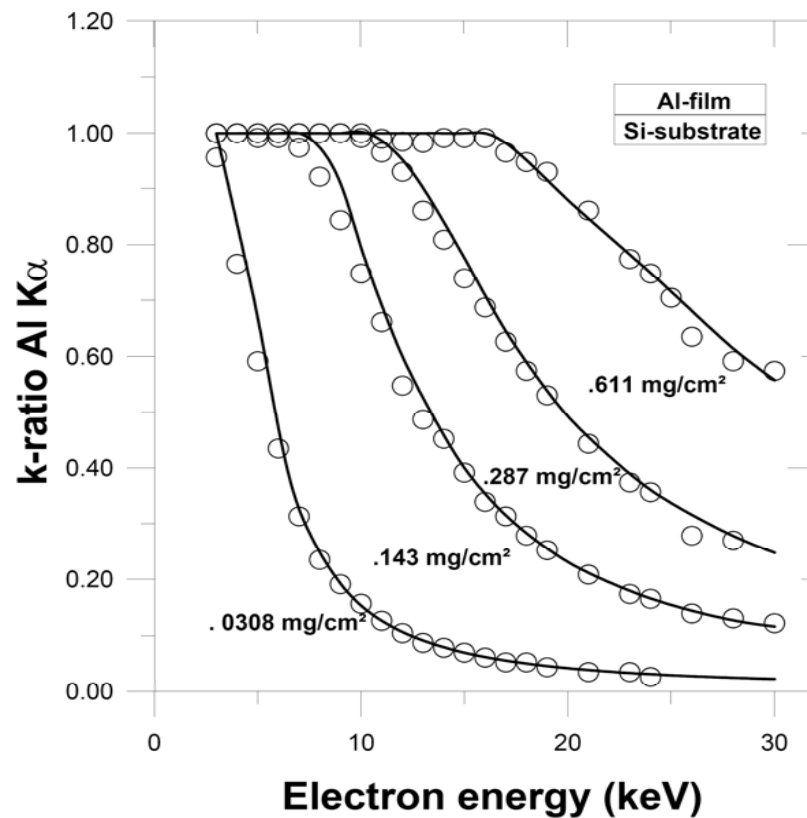
$$\delta = \rho z_m - (\zeta \chi_{ki})/2$$



Fast calculations, useful for iterative procedures involving a relatively large number of iterations.

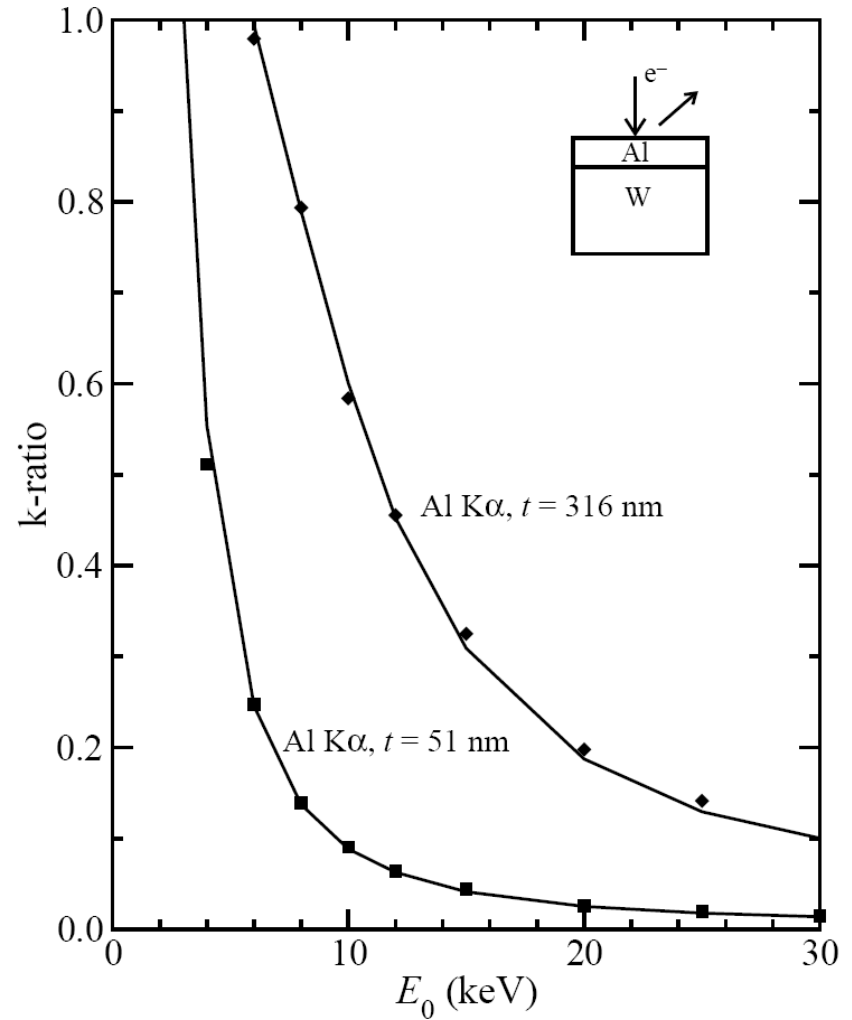
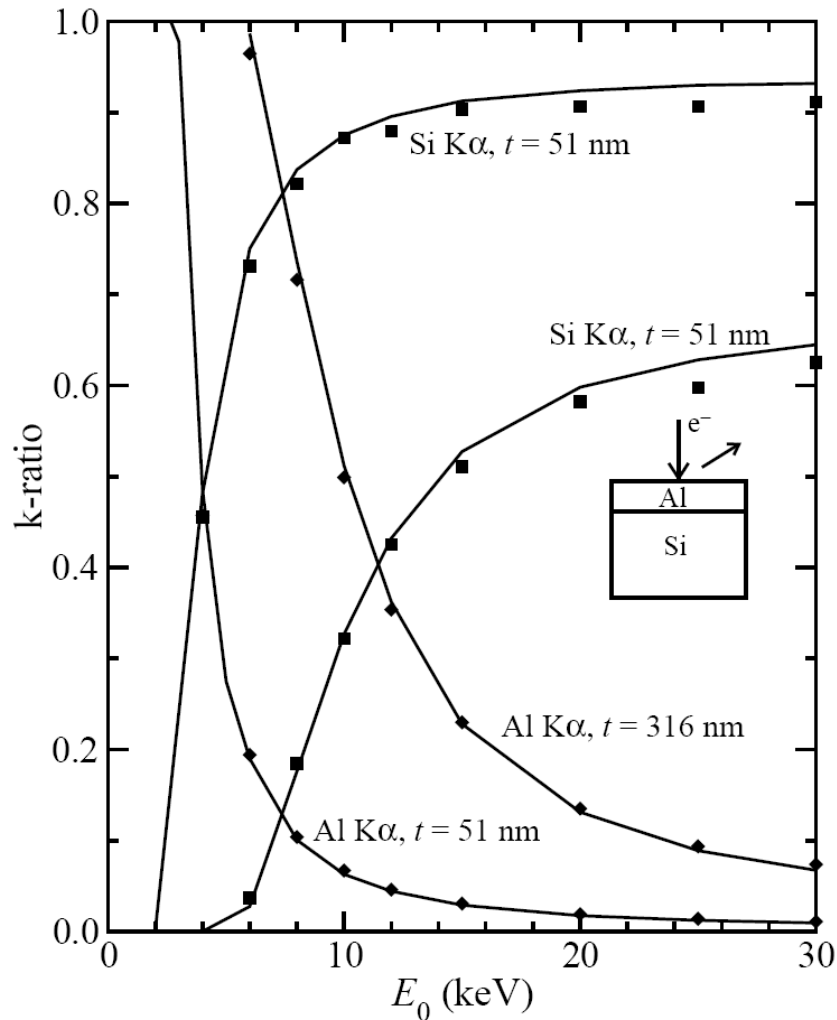
• Assessment of thin-film algorithms

- Large number of k -ratio measurements on well characterized samples available in the literature: Reuter (1978), Bastin (2000), etc..



Experimental data: Reuter *et al* (1978) and Willich & Schiffmann (1992).
Continuous line: predictions of XFILM

• Assessment of thin-film programs

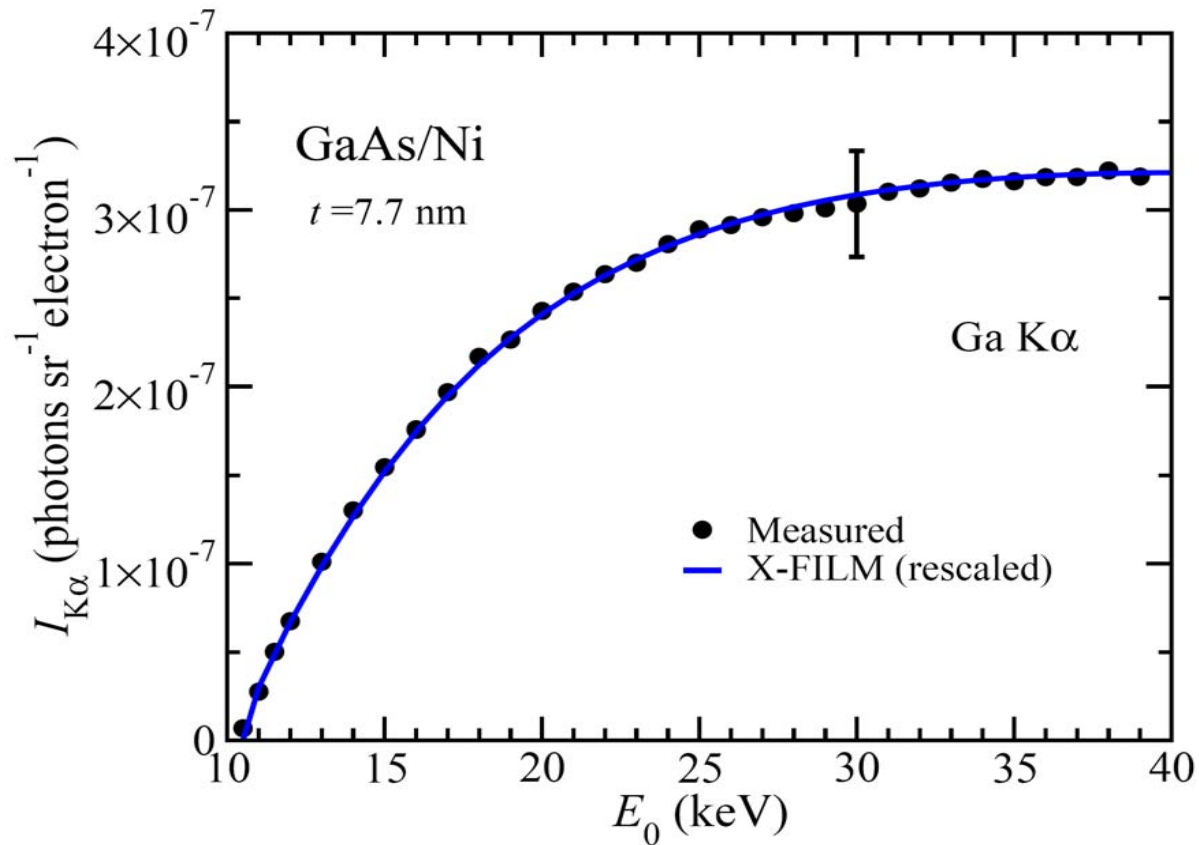


Experimental data: Bastin & Heijligers (2000)

Continuous line: Monte Carlo simulation results using PENELOPE

• Assessment of thin-film algorithms

Comparison of absolute x-ray intensities: stringent test of algorithms



Continuous line: predictions of XFILM

Stratagem - [M133.tff] - Parabolic, Fluo : L+C

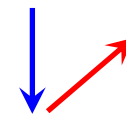
File Setup Computation Absorption Window Help

Sample Description

Layer	Element	Weight	# atoms	Mass Thick. ($\mu\text{g}/\text{cm}^2$)	Thickness (nm)	Density
1	Bi	u 0.6609	0.2095	u 26.4	264.7	1.00
	Mn	u 0.2090	0.2520			
	O	u 0.1301	0.5385			
Substrate	Sr	k 0.4774	1.0000			
	Ti	k 0.2610	1.0000			
	O	k 0.2615	3.0000			

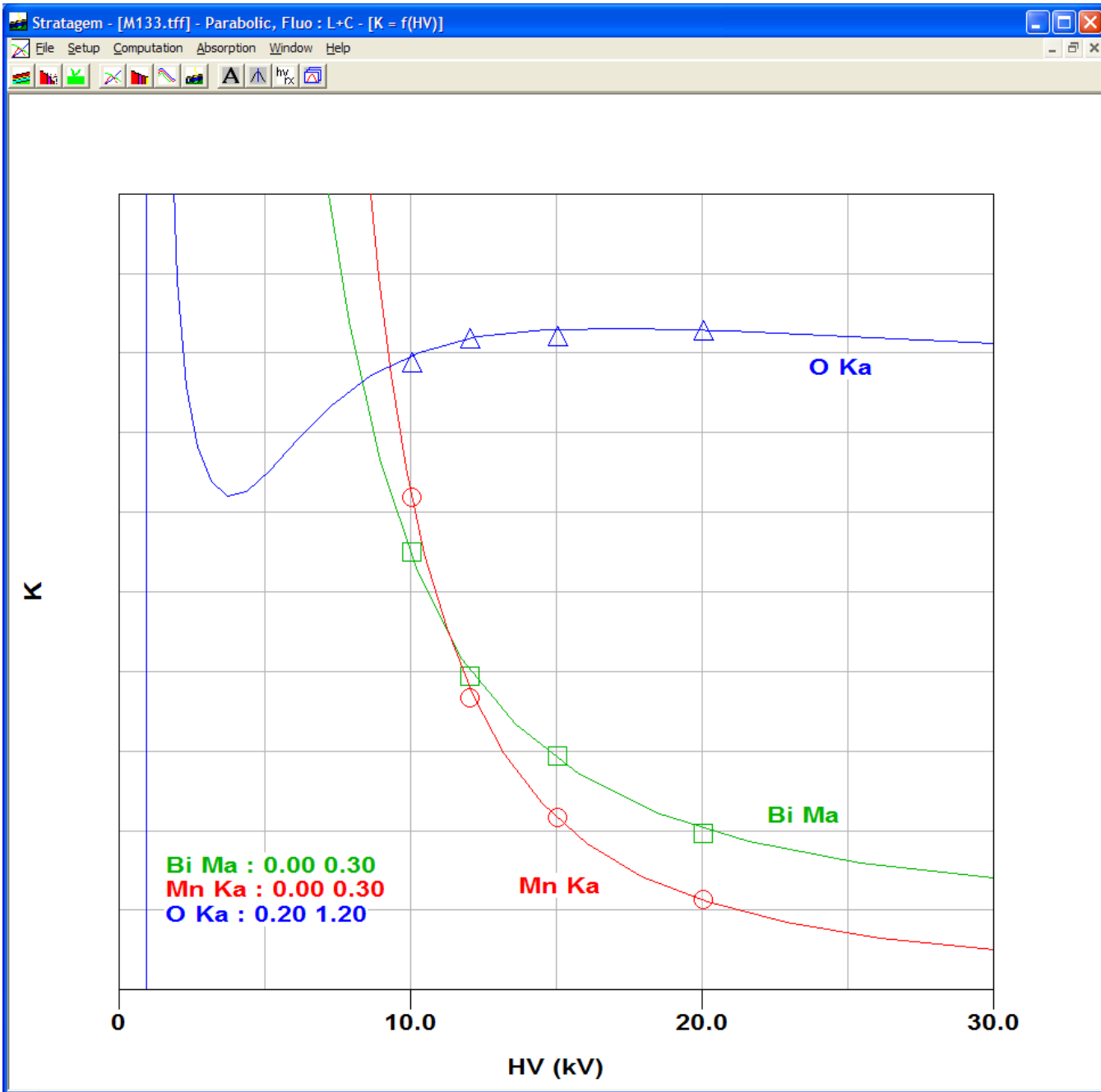
Experimental Data

anal.	Element	Line	Standard	HVstd	HVx	Ix/Istd	Kratio	Iter	Show
<input checked="" type="checkbox"/>	Bi	Ma	Bi_BiSe_	10.06	10.06	0.1650	0.0903	<input checked="" type="checkbox"/>	<input checked="" type="checkbox"/>
				12.06	12.06	0.1181	0.0644	<input checked="" type="checkbox"/>	<input checked="" type="checkbox"/>
				15.06	15.06	0.0881	0.0472	<input checked="" type="checkbox"/>	<input checked="" type="checkbox"/>
				20.05	20.05	0.0588	0.0304	<input checked="" type="checkbox"/>	<input checked="" type="checkbox"/>
<input checked="" type="checkbox"/>	Mn	Ka	Mn_Rhod	10.06	10.06	0.1858	0.0537	<input checked="" type="checkbox"/>	<input checked="" type="checkbox"/>
				12.06	12.06	0.1101	0.0328	<input checked="" type="checkbox"/>	<input checked="" type="checkbox"/>
				15.06	15.06	0.0648	0.0198	<input checked="" type="checkbox"/>	<input checked="" type="checkbox"/>
				20.05	20.05	0.0339	0.0105	<input checked="" type="checkbox"/>	<input checked="" type="checkbox"/>
<input checked="" type="checkbox"/>	O	Ka	Sr_SrTiO	10.06	10.06	0.9895	0.0871	<input checked="" type="checkbox"/>	<input checked="" type="checkbox"/>
				12.06	12.06	1.0186	0.0705	<input checked="" type="checkbox"/>	<input checked="" type="checkbox"/>
				15.06	15.06	1.0228	0.0524	<input checked="" type="checkbox"/>	<input checked="" type="checkbox"/>
				20.05	20.05	1.0500	0.0379	<input checked="" type="checkbox"/>	<input checked="" type="checkbox"/>
<input type="checkbox"/>	Sr	La	Sr_SrTiO	10.06	10.06	0.4637	0.1849	<input type="checkbox"/>	<input checked="" type="checkbox"/>
				12.06	12.06	0.8384	0.3370	<input checked="" type="checkbox"/>	<input checked="" type="checkbox"/>
				15.06	15.06	0.8672	0.3495	<input checked="" type="checkbox"/>	<input checked="" type="checkbox"/>
				20.05	20.05	0.8591	0.3431	<input checked="" type="checkbox"/>	<input checked="" type="checkbox"/>
<input type="checkbox"/>	Ti	Ka	Sr_SrTiO	10.06	10.06	0.7849	0.2001	<input checked="" type="checkbox"/>	<input checked="" type="checkbox"/>
				12.06	12.06	0.8354	0.2132	<input checked="" type="checkbox"/>	<input checked="" type="checkbox"/>
				15.06	15.06	0.8852	0.2237	<input checked="" type="checkbox"/>	<input checked="" type="checkbox"/>
				20.05	20.05	0.9237	0.2267	<input checked="" type="checkbox"/>	<input checked="" type="checkbox"/>



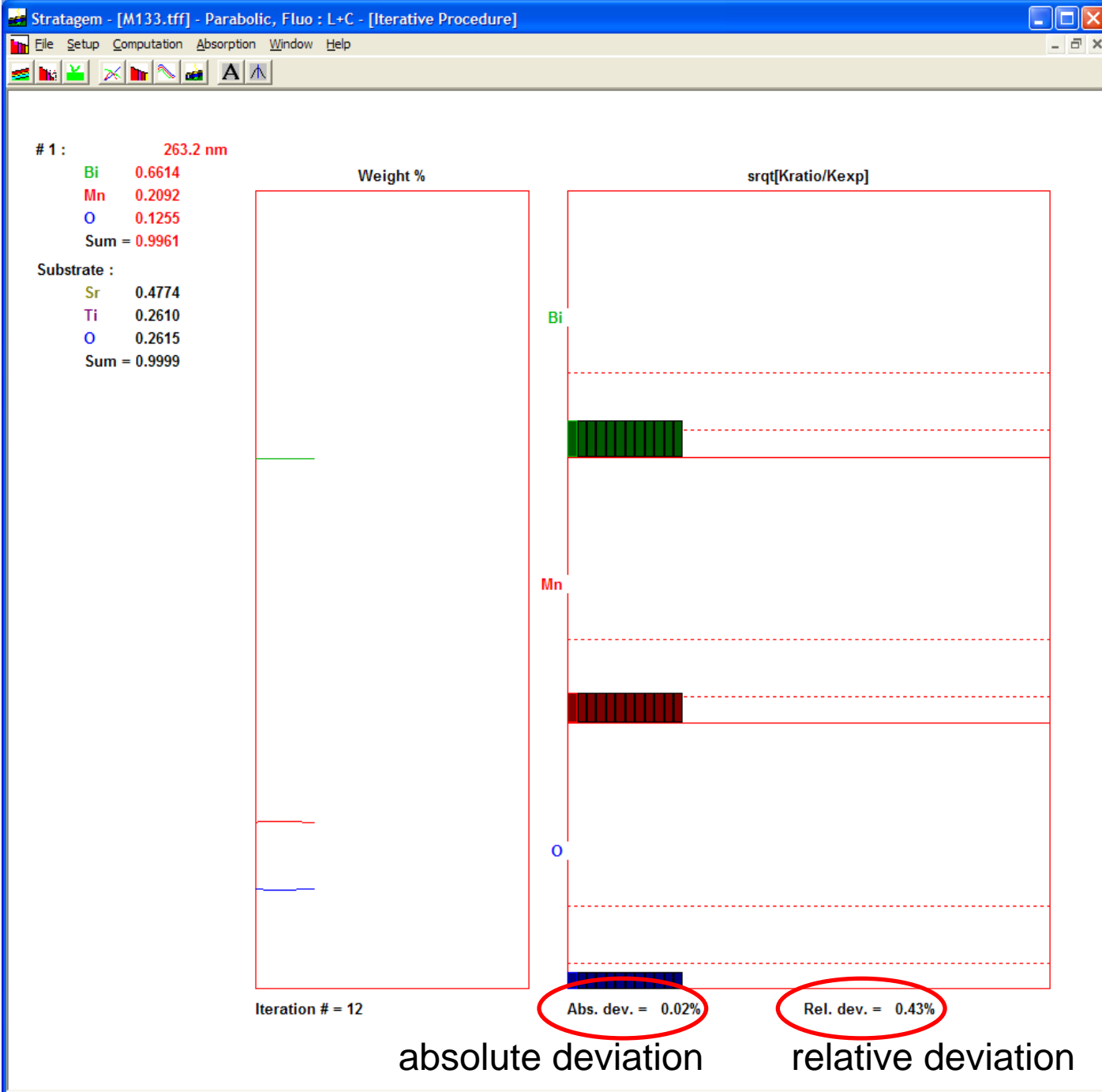
Example:
determination of thickness and composition of BiMnO₃ films on SrTiO₃ obtained by CVD

Results from STRATAgem

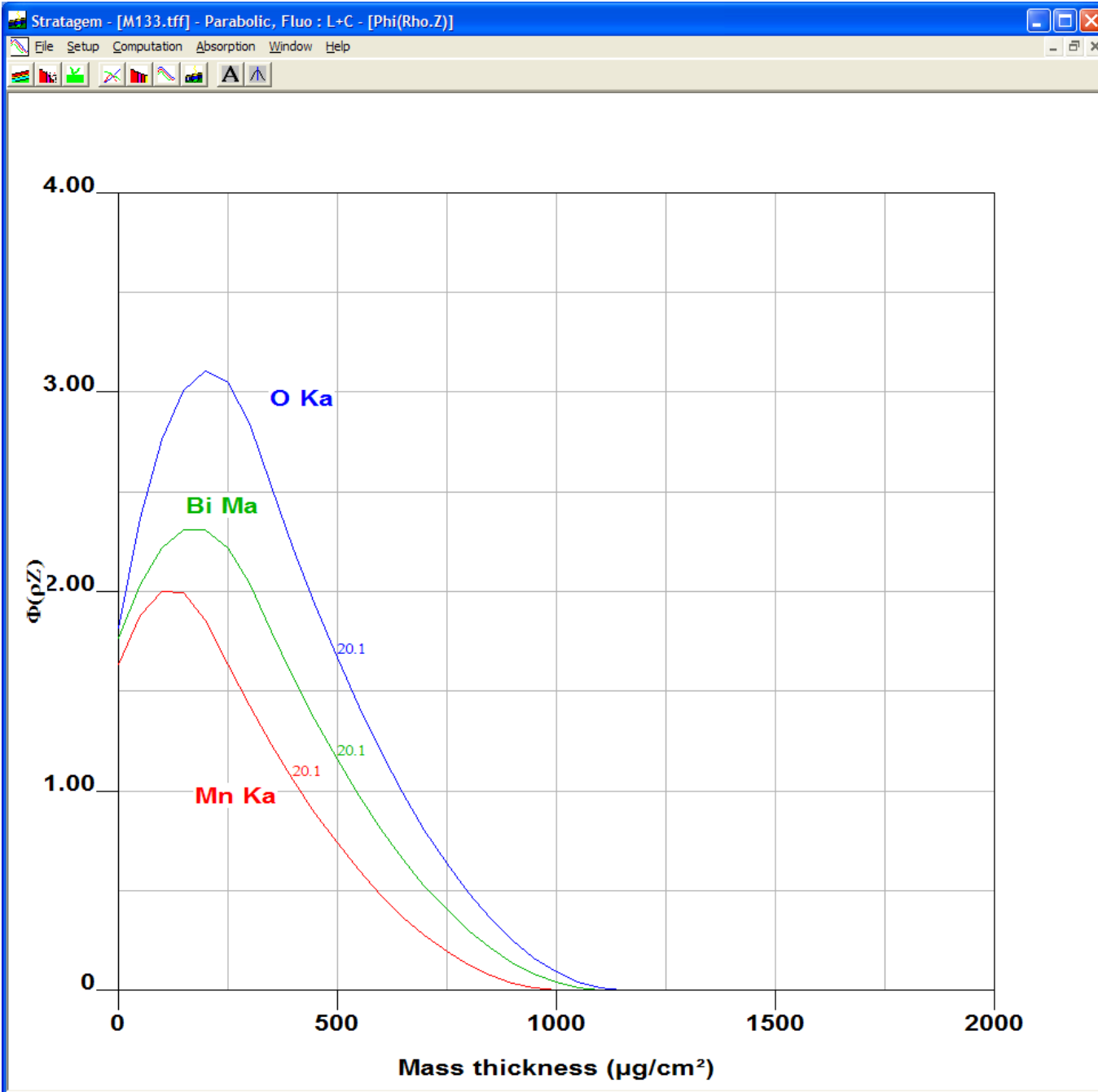


Bi = 66.1 wt.%
Mn = 20.9 wt.%
O = 12.55 wt.%
 $t = 26.4 \mu\text{g}/\text{cm}^2$

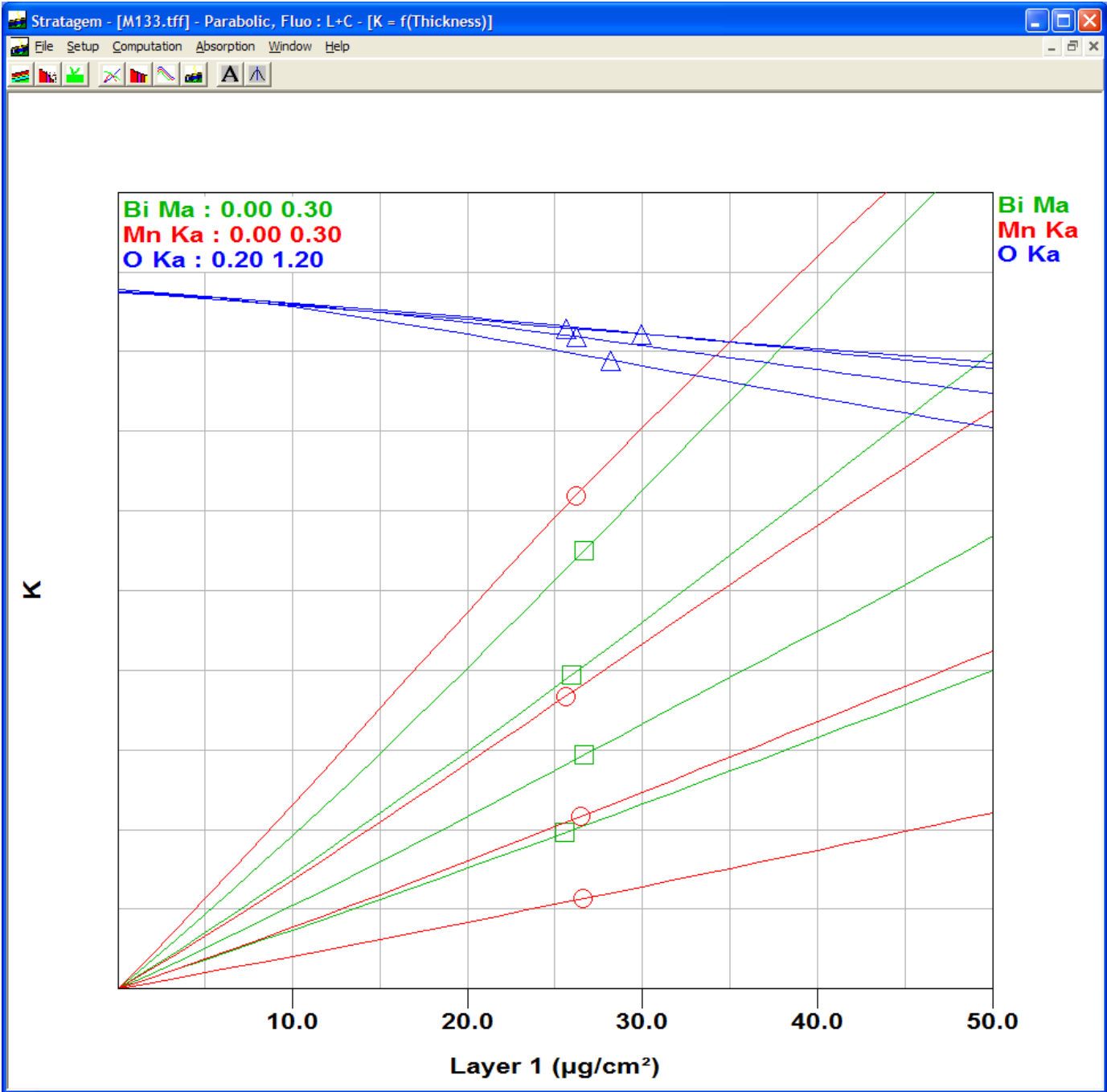
Comparison of the experimental k -ratios as functions of the incident electron energy with the predictions of the thin-film program for the estimated thickness and composition



Iterative process with the estimated concentrations and thickness and errors



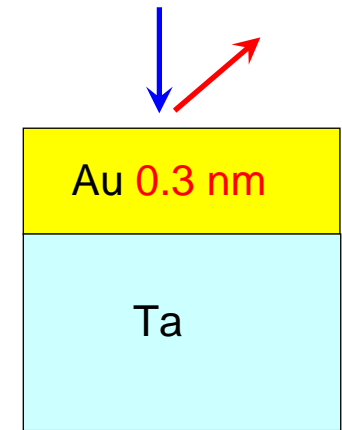
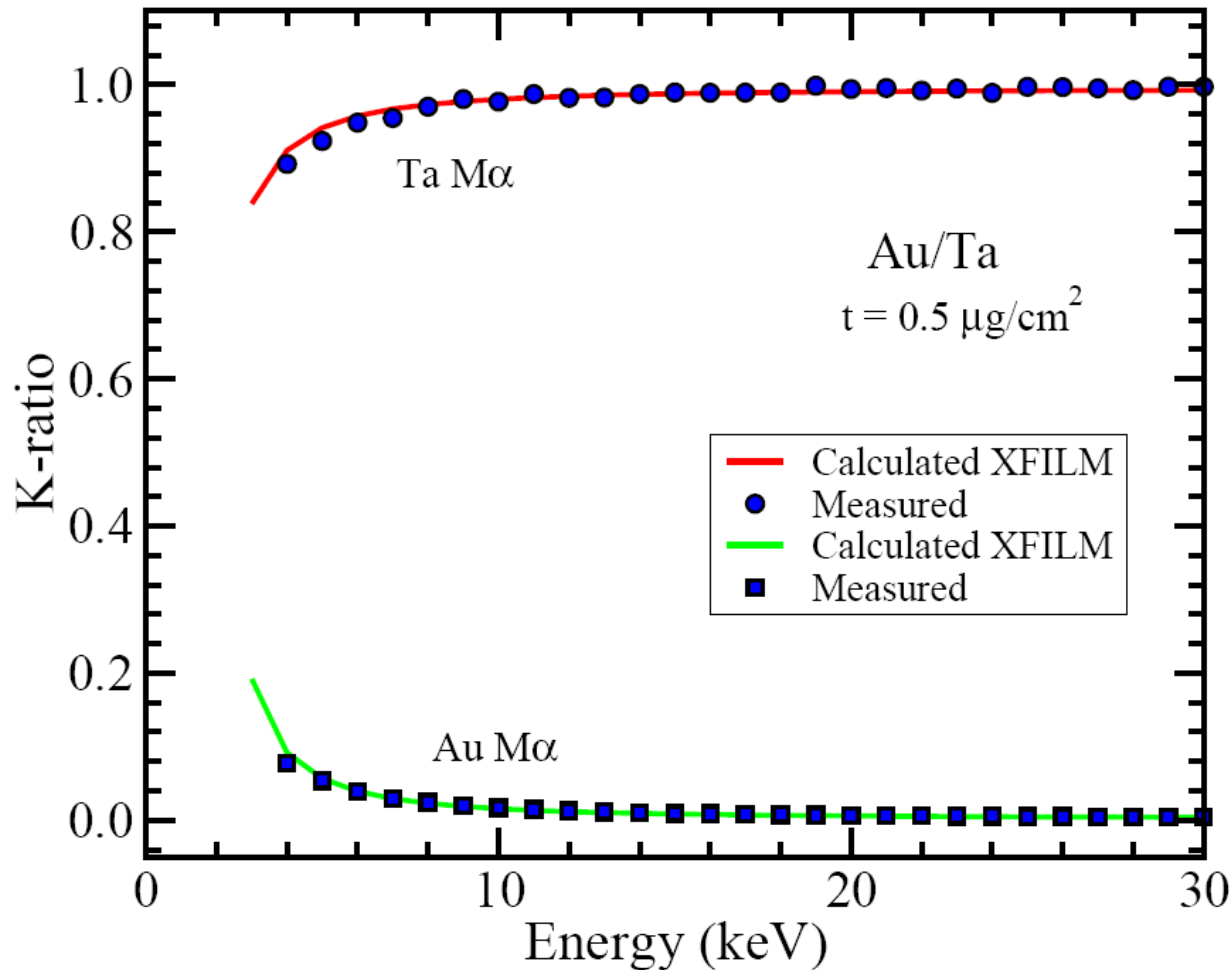
Depth-distribution
of ionizations for
the measured
elements at 20
keV



Bi = 66.1 wt.%
 Mn = 20.9 wt.%
 O = 12.55 wt.%
 $t = 26.4 \mu\text{g}/\text{cm}^2$

Comparison of the k-ratio as a function of the estimated mass thickness for each energy

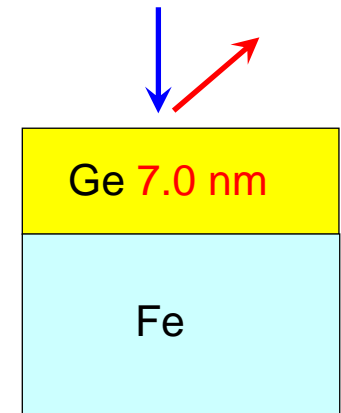
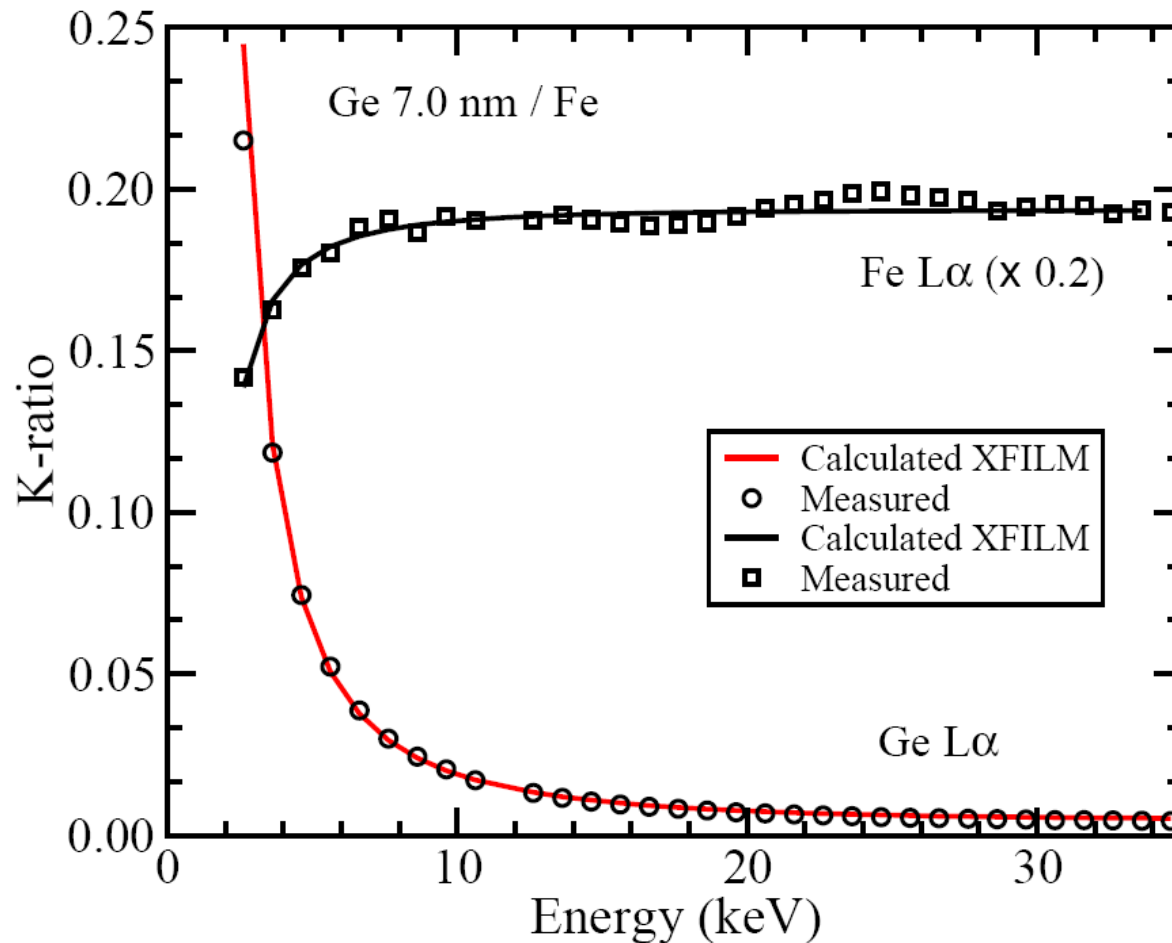
• Au/Ta



Unknown:
film thickness

- Accuracy depends on number of measurements and x-ray lines used
- Similar difficulties to those found in trace element analysis
- Excellent sensitivity to surface layers

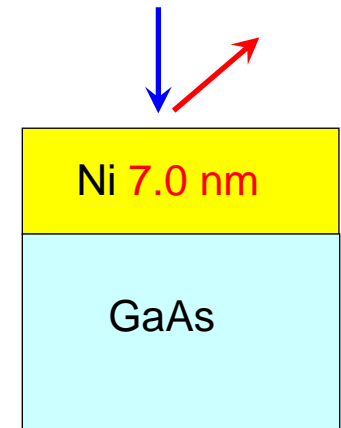
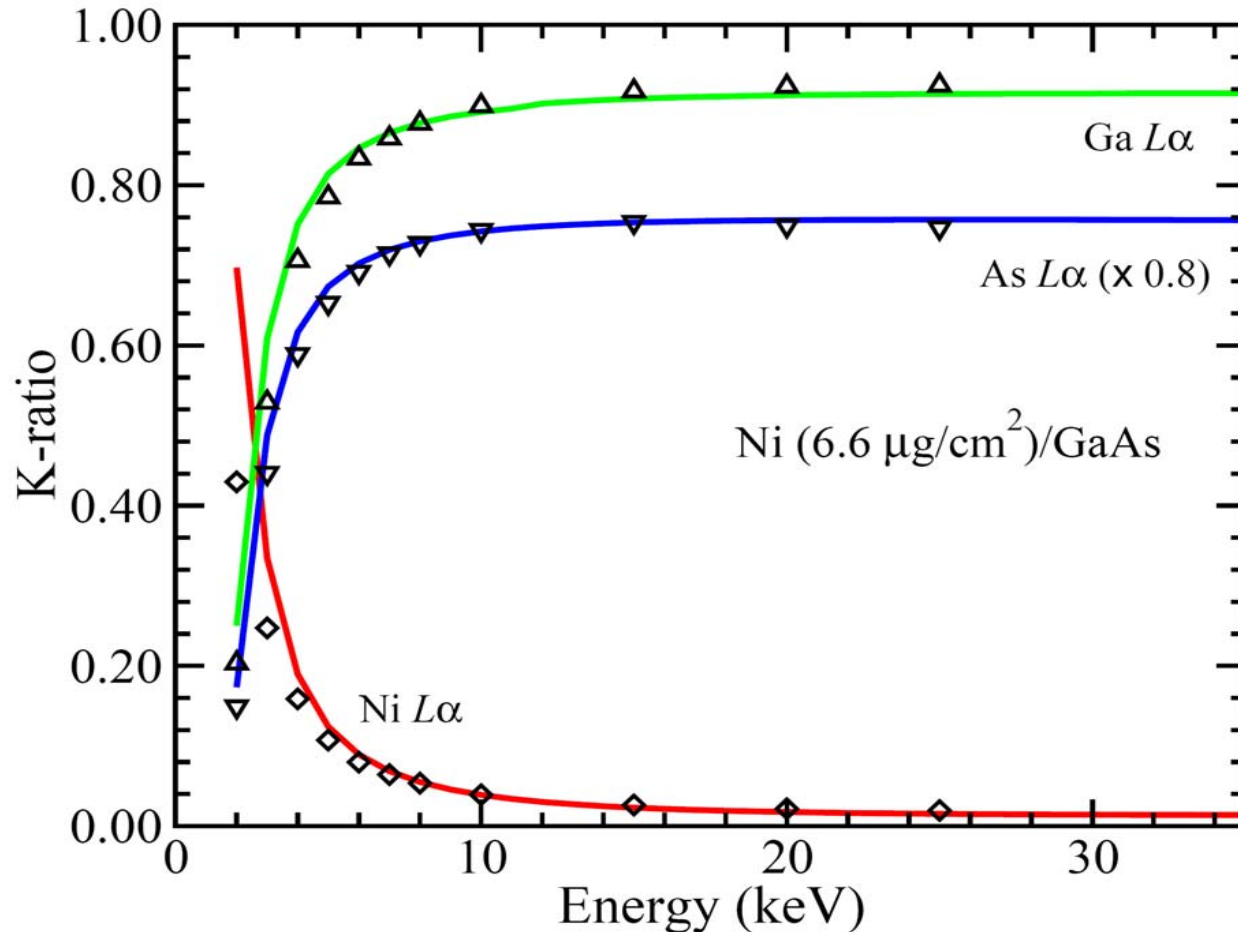
• Ge/Fe



Unknown:
film thickness

- Optimal choice of accelerating conditions depends on thickness
- Good accuracy achieved in part due to similar Z

• Ni/GaAs

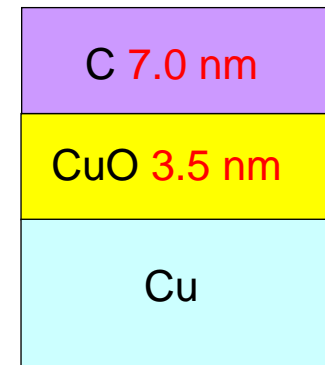
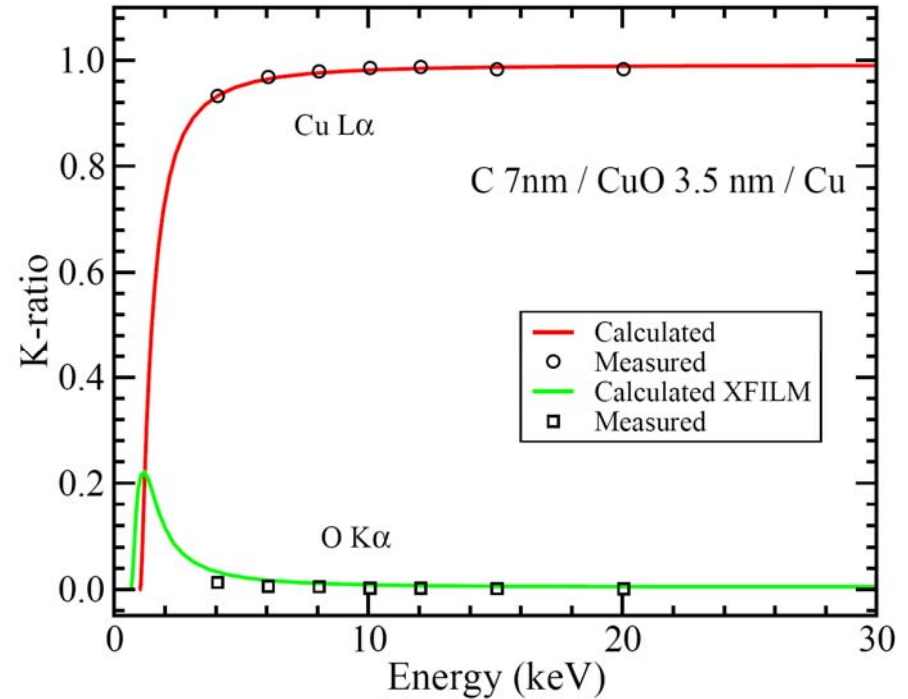
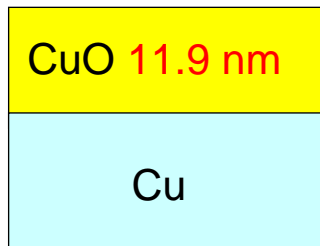
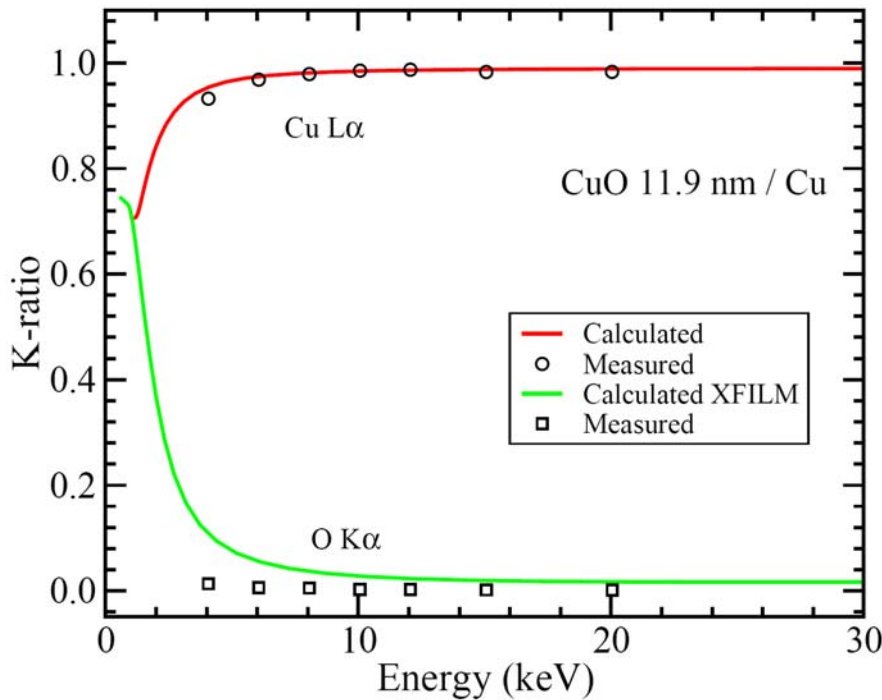


Unknown: film thickness

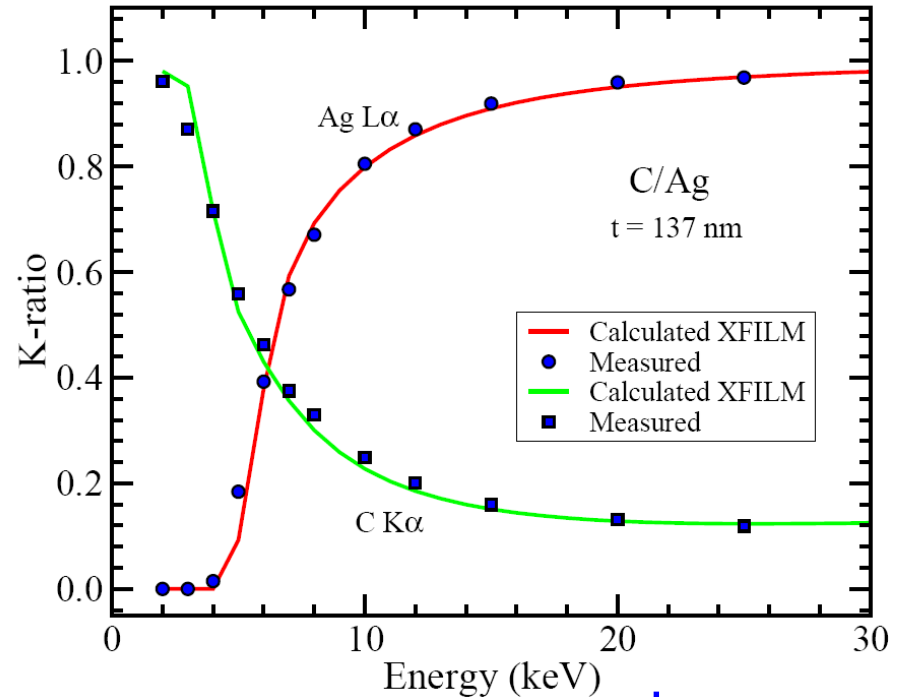
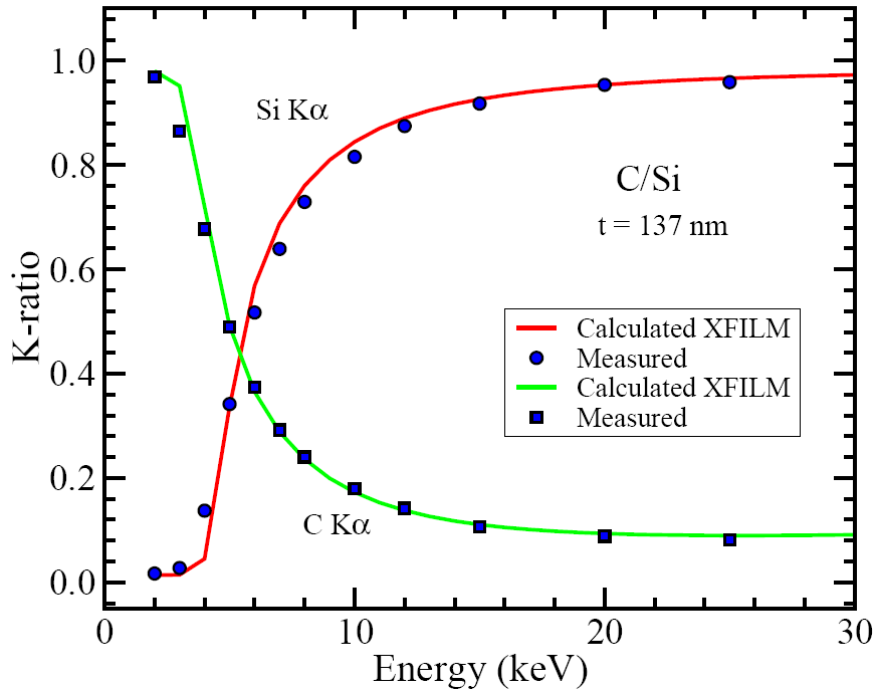
- Influence of surface contamination: native oxide layer, carbon, Si, etc..
- Accuracy may also depend on conditions of the standards

• Cu oxide films

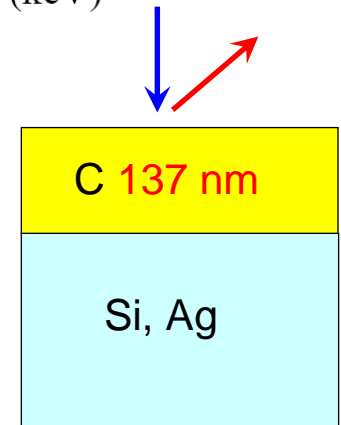
- Measurements from substrate elements useful to check consistency
- Agreement improves by assuming a C layer on top



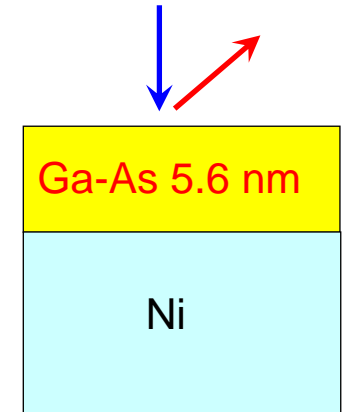
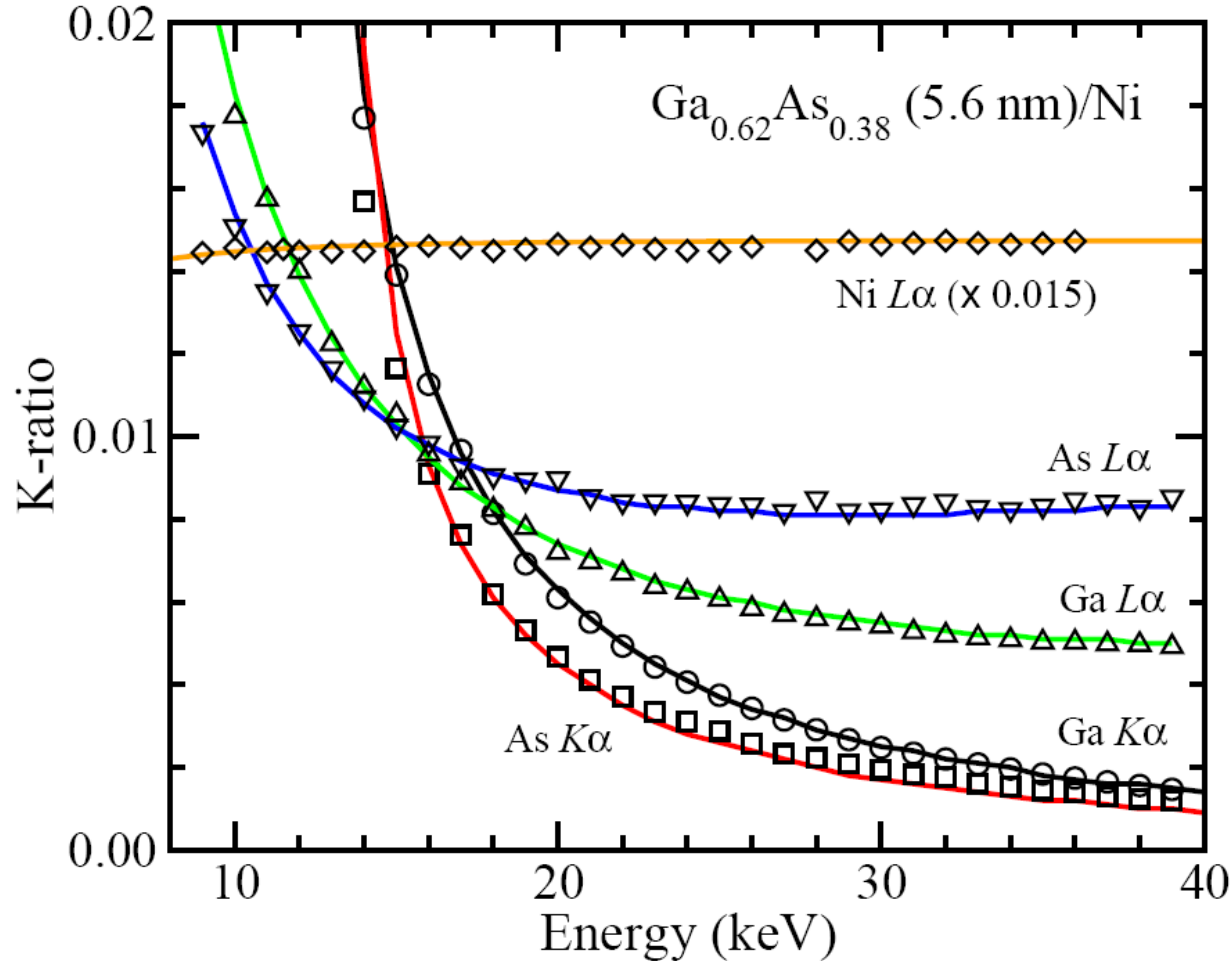
• Carbon films on several substrates



- Films obtained simultaneously (same thickness) by evaporation
- Good agreement even for large differences in Z



• Ga-As/Ni

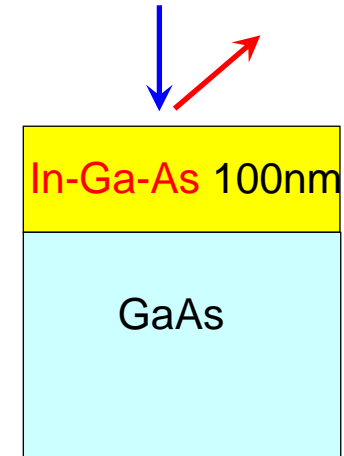
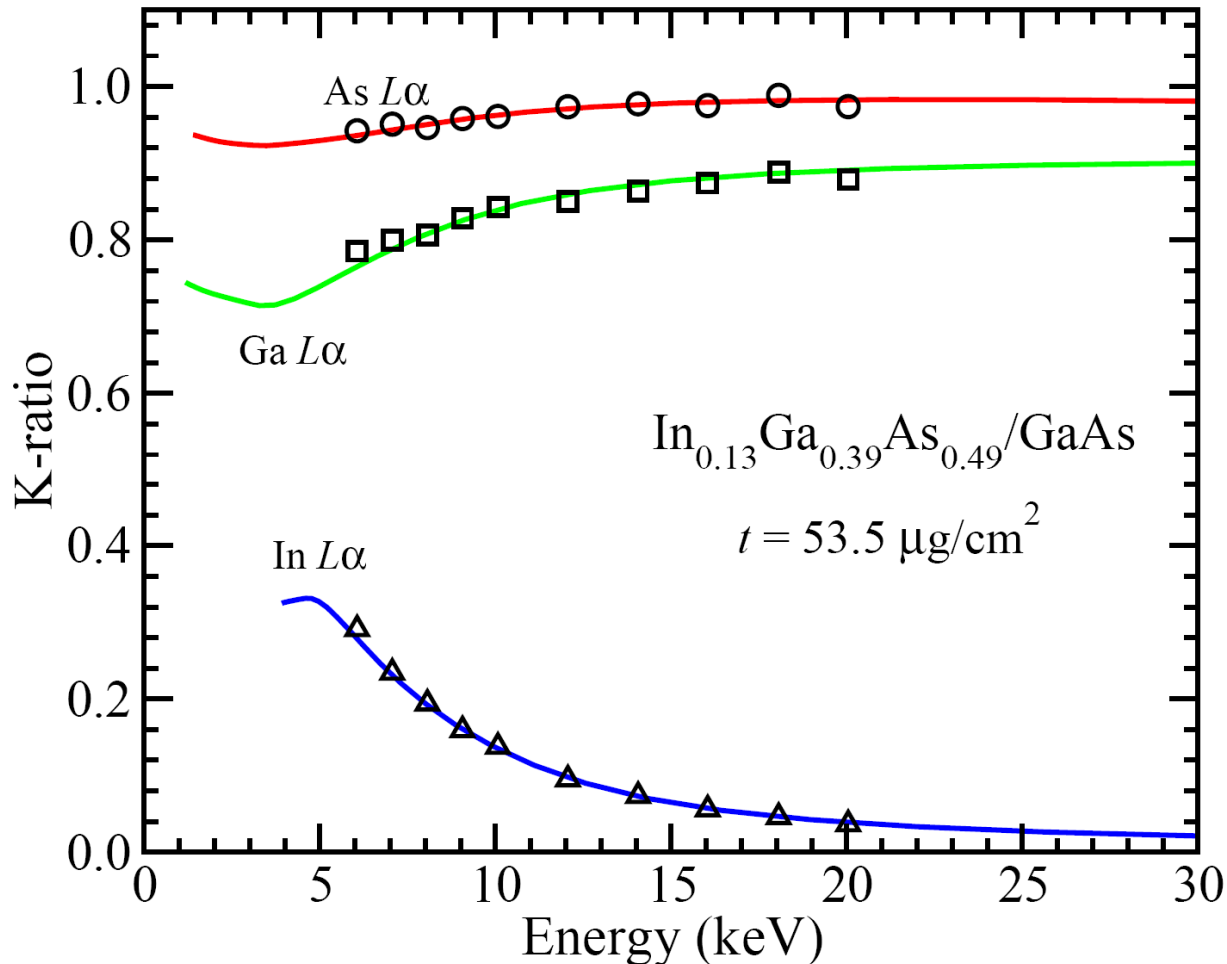


Unknown: film thickness and composition

- Measurements using different x-ray lines (film and substrates elements) not required but useful to check consistency.

● In-Ga-As/GaAs

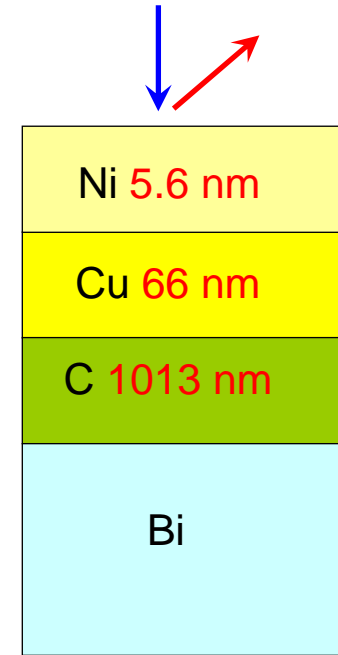
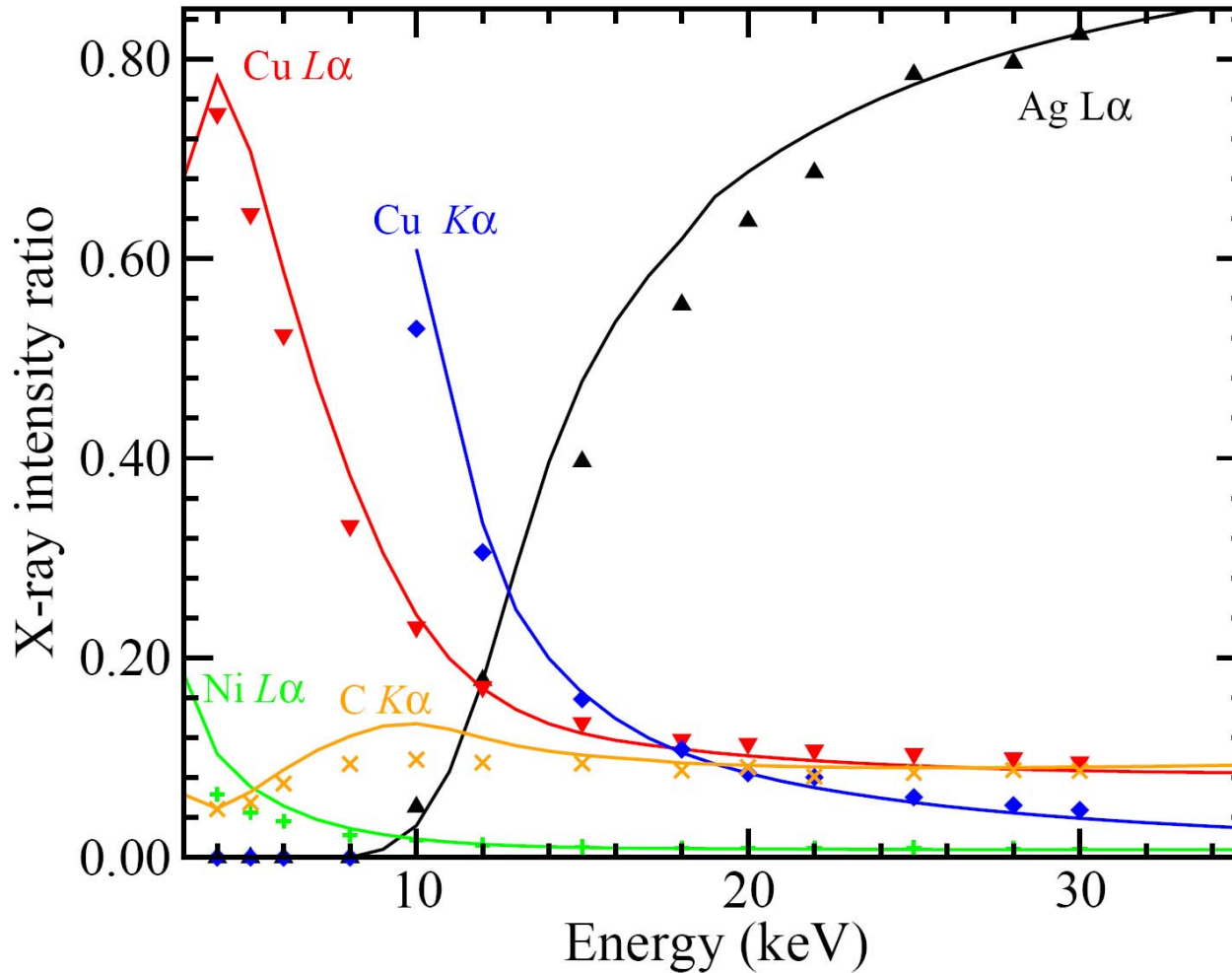
Continuous line: STRATagem



Unknown:
film composition

- Elements present simultaneously in both film and substrate
- Thickness obtained by other techniques

• Ni/Cu/C/Ag



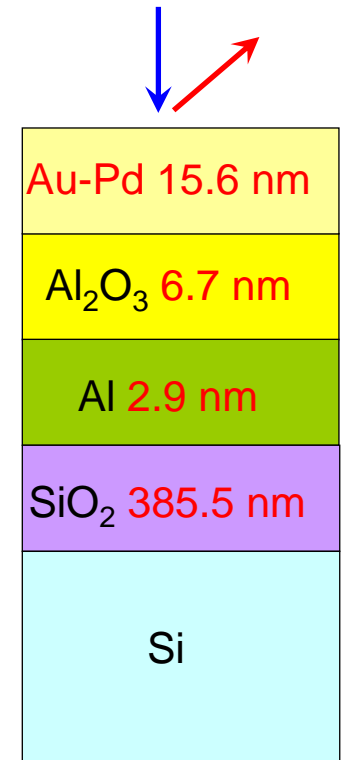
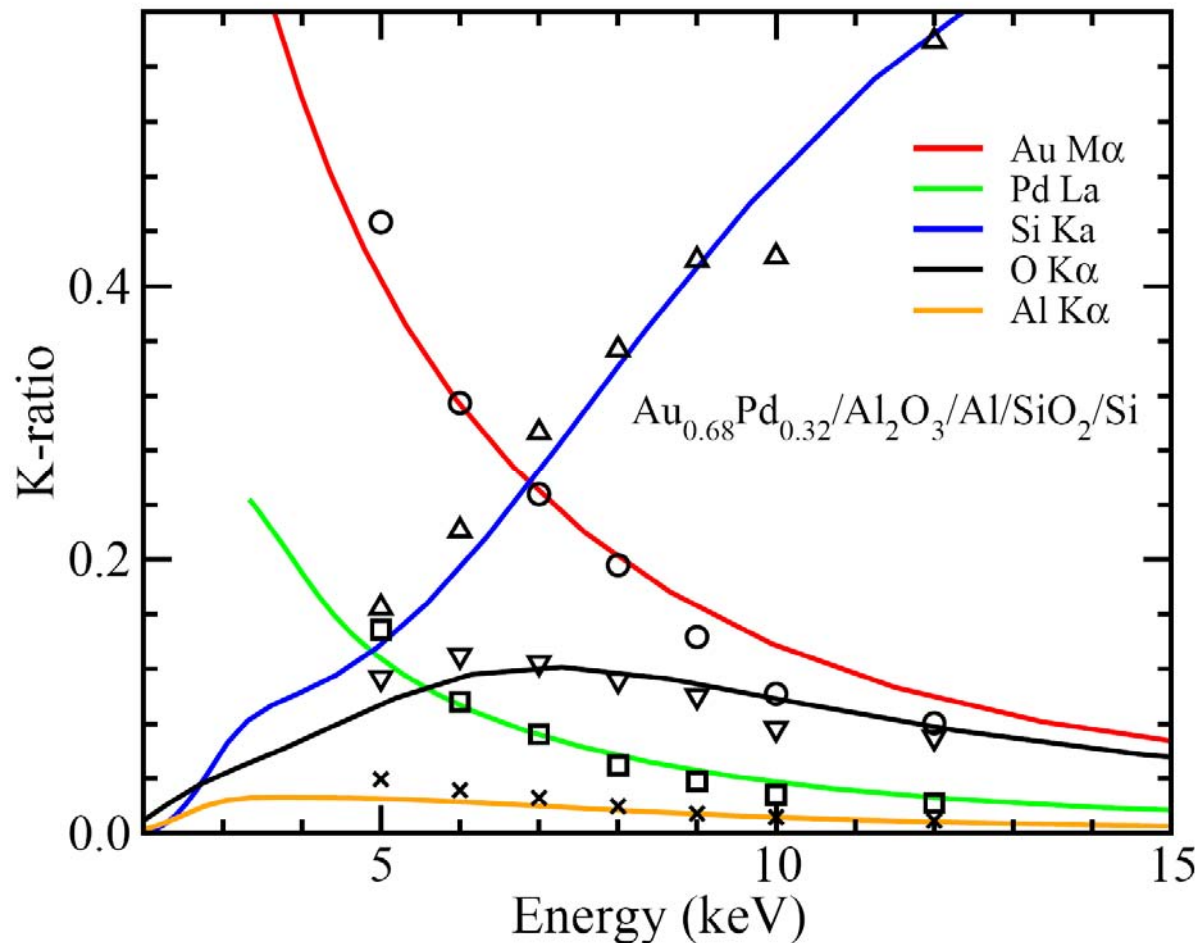
Unknown:
thicknesses

• Accuracy may vary depending on the particular case

Continuous line: X-FILM

• Au-Pd/Al₂O₃/Al/SiO₂/Si

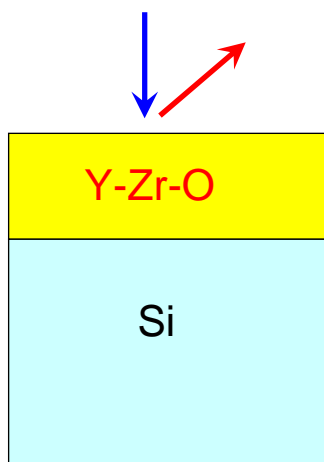
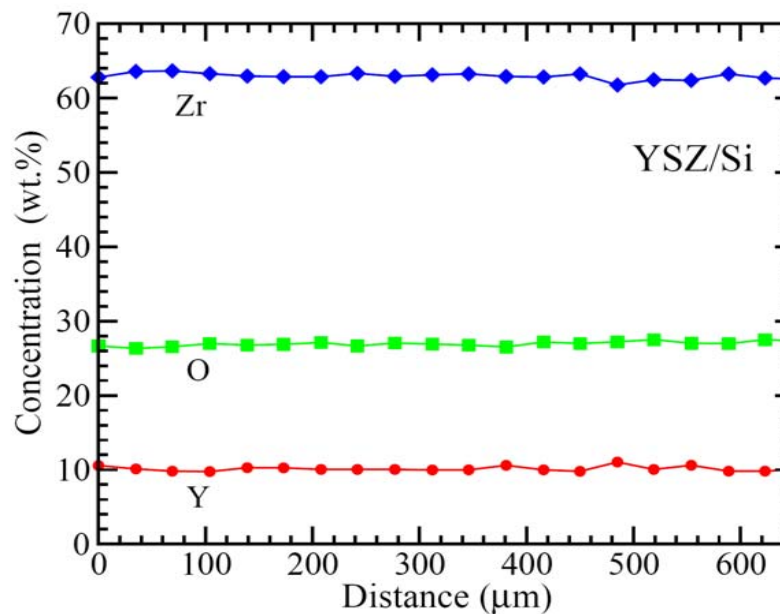
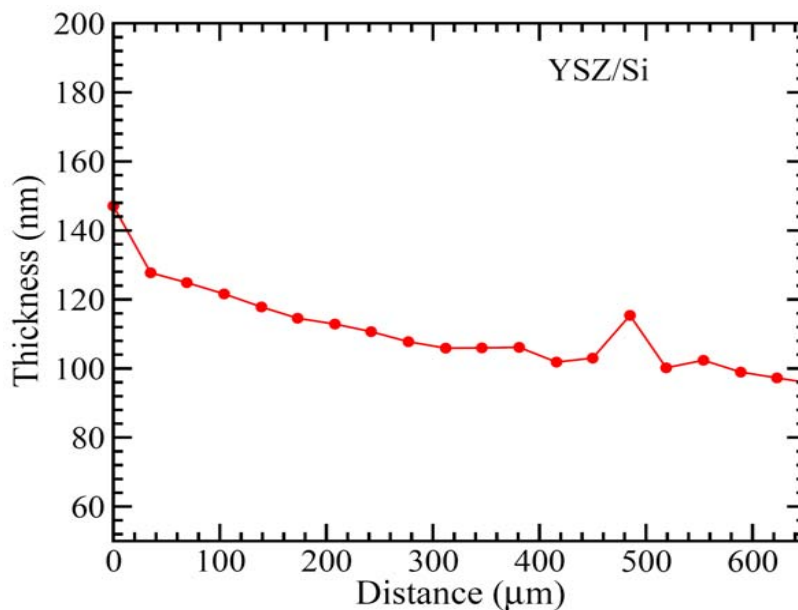
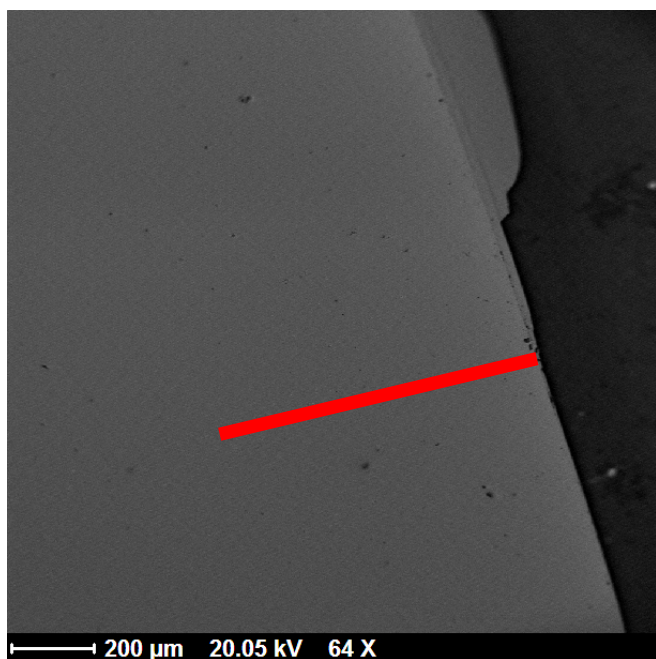
Experimental measurements: E. Heikinheimo
 Continuous line: STRATagem



Unknown:
 Au-Pd composition
 & layers thickness

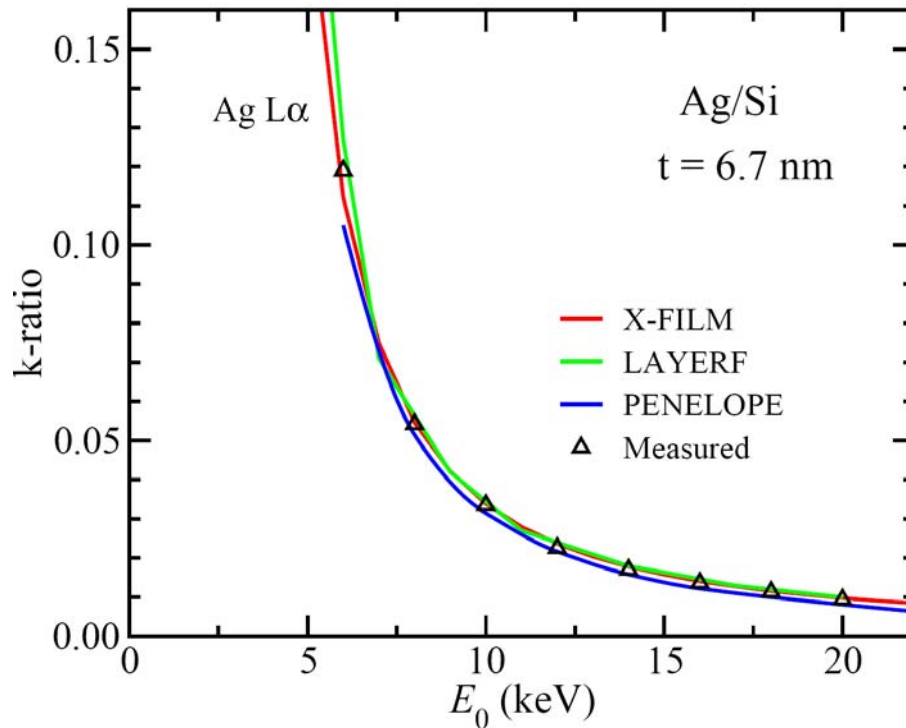
- Sample structure required if elements present in different layers
- Alternatively, solution by trial-error mode (graphical interface)

• Lateral resolution of thickness & composition



Results obtained by using STRATAline

• Comparison with other thin-film programs & techniques



- Campos *et al.* (1999): thickness difference < 5% for very thin films on Si from different approaches (quartz crystal, LAYERF, X-FILM, PENELOPE)

Layer element	Thickness (nm)					
	Quartz crystal	LAYERF L α	LAYERF M α	X-FILM L α	X-FILM M α	PENELOPE
Ge	6.8 (0.2)	6.9 (0.3)	-	6.6 (0.3)	-	6.6 (0.4)
Ag	6.7 (0.3)	6.8 (0.3)	-	6.7 (0.1)	-	6.9 (0.3)
Sn	6.4 (0.4)	6.3 (0.1)	-	6.2 (0.1)	-	6.1 (0.2)
Au	7.1 (0.2)	7.0 (0.2)	7.0 (0.2)	7.0 (0.1)	7.2 (0.1)	6.9 (0.7)

● Conclusions

- It is possible to determine the composition and thickness of thin films and multilayers non-destructively by EPMA
- The technique requires measurements at varying incident electron energies and analysis of measured *k*-ratios by means of a thin-film program
- High sensitivity for detecting surface layers (thickness of $0.1 \mu\text{g}/\text{cm}^2$)
- Thin films on substrates. Thicknesses and compositions with accuracy better than 5% can be routinely obtained
- Difficulties for complex multilayers if elements are present in different layers and/or x-rays from buried layers are strongly attenuated. Accuracy depend on each particular case.
- Lateral resolution of the order of 1 micron

EPMA is a versatile tool for thin-film analysis, supplementing the information obtained from conventional surface-analytical techniques (SIMS, AES, XPS..)